



Call: H2020-SC5-2014-two-stage

Topic: SC5-01-2014

PRIMAVERA

Grant Agreement 641727



PRocess-based climate sIMulation: AdVances in high resolution modelling and European climate Risk Assessment

Deliverable D2.3

Quantification based on WP2 findings and initial sensitivity experiments in WP3

Deliverable Title	<i>Quantification based on WP2 findings and initial sensitivity experiments in WP3</i>		
Brief Description	<i>Based on WP2 findings and initial sensitivity experiments performed in WP3, quantification of the relative merits of increased resolution and model developments of the North Atlantic, Arctic, Pacific and tropical climates and their robustness across the PRIMAVERA models to provide recommendations to WP6 for the Stream 2 design.</i>		
WP number	2		
Lead Beneficiary	CMCC		
Contributors	<i>Alessio Bellucci (CMCC) Daniele Peano (CMCC) Xavier Levine (BSC) Eduardo Moreno (BSC) Louis-Philippe Caron (BSC) Federico Fabiano (CNR) Virna Meccia (CNR) Susanna Corti (CNR) Sarah Keeley (ECMWF) Richard Bintanja (KNMI) Oliver Gutjahr (MPI-M) Johann Jungclaus (MPI-M) Adrian New (NOCS) George Nurser (NOCS) Torben Koenigk (SMHI) Kristian Stommelen (UOXF) Hannah Christensen (UOXF) Nicolas Bellouin (UREAD) Omar Muller (UREAD) Pier Luigi Vidale (UREAD)</i>		
Creation Date			
Version Number			
Version Date			
Deliverable Due Date	28/2/2019		
Actual Delivery Date			
Nature of the Deliverable	R 	<i>R - Report P - Prototype D - Demonstrator O - Other</i>	
Dissemination Level/ Audience	PU 	<i>PU - Public PP - Restricted to other programme participants, including the Commission services RE - Restricted to a group specified by the consortium, including the Commission services CO - Confidential, only for members of the consortium, including the Commission services</i>	

Version	Date	Modified by	Comments

Table of Contents

1. Executive Summary.....	5
2. Project Objectives.....	7
3. Detailed Report.....	8
3.1 <i>Objectives and methodology</i>	8
3.2 Ocean	9
3.3 Sea-Ice	18
3.4 Atmosphere	29
3.5 Land	32
3.6 Stochastic Physics	36
4. Lessons Learnt.....	47
4.1. The relative merits of enhanced model resolution versus model developments on bias reduction.....	47
4.2 A note on recommendations for Stream 2.....	48
5. Links Built.....	49

1. Executive Summary

The focus of this deliverable is on the quantification of the relative merits of enhanced horizontal resolution and improved physical parameterizations in the representation of the climate over key areas of the Earth, including the North Atlantic, North Pacific, Arctic and tropical regions in the PRIMAVERA models ensemble.

A significant aspect emerging from the analyses presented in this report is the strong regional and process dependence of the relative benefits of resolution and improved physics. The main results are summarized below.

Ocean

Biases in the upper thermal structure of the North Atlantic (SST and stratification) appear to benefit more from a resolution increase, than from the use of more sophisticated vertical mixing schemes (IDEMIX and OSMOSIS; 3.2.1 and 3.2.2, respectively). However, the opposite is true for the Southern Ocean, where the use of the OSMOSIS mixing scheme is found to significantly alleviate a long-lasting warm austral summer SST bias (3.2.2), which, on the other hand, appears to be relatively insensitive to increases in the resolution (Hewitt et al., 2016). In another analysis (3.3.2), changes in a set of ocean model parameters (affecting, among other aspects, the penetration of turbulent kinetic energy below the mixed layer and the Langmuir cells representation) are conducive to a systematic reduction in the integrated ice edge error over the Arctic, while increasing resolution yields a more uncertain result.

Sea-ice

In general terms, the assessment of the relative impacts of resolution enhancement and improved physics yields more elusive results. This is the case of the analysis presented in section 3.3.1, testing the inclusion of Arctic melt ponds against the increase of model resolution. According to this set of results, melt ponds and increased resolution lead to a similar improvement of sea ice concentrations in the Barents Sea and a reduced cold bias in the near-surface temperatures over the Arctic. Analogous indications of a substantially equivalent impact of model physics and resolution on the representation of the Arctic climate can be drawn from the analyses presented in section 3.3.3. However, significant differences emerge when looking at the European surface climate, with a more pronounced impact of resolution.

Atmosphere

A case study providing a particularly clear response to the primary issue addressed by D2.3, is the analysis presented in section 3.4.1, focusing on the hydrological cycle over the Arctic. Here it is shown how a refined representation of the snowfall ratio (the ratio of snowfall to total precipitation) can lead to a stronger improvement compared to the mere increment of model resolution.

An intriguing aspect emerging for a specific subset of the analysed physical processes, is the potential interdependency of model resolution and physics complexity. This is the case for radiative fluxes, clouds, and aerosol-cloud interactions (3.4.2). There are benefits from increasing resolution for simulating clouds, aerosols, and radiation, but those benefits may require very high resolutions to fully appear. Those benefits are also modulated by the complexity in model physics. Complex cloud microphysics help make the most of very high resolutions (e.g., in terms of simulating cloud water content in extra-tropical cyclones). Similarly, simplifying the representations of aerosol-cloud interactions offsets some of the gains of increasing resolution when simulating cloud cover and albedo.

Land

Preliminary sensitivity tests performed on two different land-surface models (JULES and CLM; 3.5.1) by changing soil boundary conditions, river routing schemes (either in resolution or complexity) and forcing fluxes, provide indications of a positive impact from improved boundary conditions and physics, while no sizeable impact from resolution increases. These aspects will be further analysed in the context of Stream 2 simulations.

Stochastic Physics

The analysis of the relative impact of stochastic physics versus increased resolution (3.6) contributes to enlarge the scope of D2.3 beyond the mere enhancement of physics complexity via the inclusion of more sophisticated (compared to standard model configurations) physical parameterizations.

The analyses presented in section 3.6.1 show that in several respects (mean state changes and European extreme events), stochastic physics can mimic the impact of increased resolution. However, the amplitude of change is sometimes smaller with stochastic physics, suggesting that the schemes may need further tuning to represent the sub-grid scale processes with better fidelity. On the other hand, increased resolution can sometimes deteriorate the model (as with the jet latitude structure) in ways that stochasticity appears not to. The representation of winter weather regime patterns in the North Atlantic (3.6.2) exhibits a slight improvement associated with increased resolution, while a similar bias reduction is only achieved when stochastic physics is applied to the atmospheric component, while a worsening of the biases is obtained when ocean stochastic physics is used. Overall, stochasticity remains a promising avenue for improving climate models, but a robust assessment of its merits with respect to resolution will require large-sized ensembles of simulations to verify the significance of the detected differences against the intra-ensemble variability.

Concluding remarks

At this stage it is clearly not possible to rank, in absolute terms, the benefits of resolution versus model improvements (and stochastic physics) since these may all potentially contribute to reduce regional biases, depending on the specific study area, process under exam, and model in use.

It is also important to remark that the set of results presented in this report should be considered as a starting point for more in-depth analyses of the relative benefits of model improvements as compared to resolution increase. Such analyses will greatly benefit from a coordinated, protocol-driven, set of coordinated experiments with a wide blend of different climate models testing selected physical parameterizations across a hierarchy of model resolutions. An additional key element to be considered when designing this kind of efforts is the “adjustment timescale” associated with the set-up of specific physics improvements: certain processes may take several decades to manifest themselves in the model climatology (e.g., slow ocean circulation response to changes in the vertical mixing), pointing to the need for adequately extended (multi-decadal) sensitivity experiments.

2. Project Objectives

With this deliverable, the project has contributed to the achievement of the following objectives (DOA, Part B Section 1.1) WP numbers are in brackets:

No.	Objective	Yes	No
A	To develop a new generation of global high-resolution climate models. (3, 4, 6)	Yes	
B	To develop new strategies and tools for evaluating global high-resolution climate models at a process level, and for quantifying the uncertainties in the predictions of regional climate. (1, 2, 5, 9, 10)	Yes	
C	To provide new high-resolution protocols and flagship simulations for the World Climate Research Programme (WCRP)'s Coupled Model Intercomparison Project (CMIP6) project, to inform the Intergovernmental Panel on Climate Change (IPCC) assessments and in support of emerging Climate Services. (4, 6, 9)		No
D	To explore the scientific and technological frontiers of capability in global climate modelling to provide guidance for the development of future generations of prediction systems, global climate and Earth System models (informing post-CMIP6 and beyond). (3, 4)	Yes	
E	To advance understanding of past and future, natural and anthropogenic, drivers of variability and changes in European climate, including high impact events, by exploiting new capabilities in high-resolution global climate modelling. (1, 2, 5)		No
F	To produce new, more robust and trustworthy projections of European climate for the next few decades based on improved global models and advances in process understanding. (2, 3, 5, 6, 10)	Yes	
G	To engage with targeted end-user groups in key European economic sectors to strengthen their competitiveness, growth, resilience and ability by exploiting new scientific progress. (10, 11)		No
H	To establish cooperation between science and policy actions at European and international level, to support the development of effective climate change policies, optimize public decision making and increase capability to manage climate risks. (5, 8, 10)		No

3. Detailed Report

3.1 Objectives and methodology

The focus of this deliverable is on the quantification of the relative merits of enhanced horizontal resolution and improved physical parameterizations (hereafter, IP) in the representation of the climate over key areas of the Earth, including the North Atlantic, North Pacific, Arctic and tropical regions in the PRIMAVERA models ensemble. The influence of horizontal resolution (stand-alone) has been extensively documented in D2.1 and D2.2, addressing the role of the ocean and atmospheric model resolution, respectively, using both results from WP6 Stream 1 and a set of prototype simulations (the so-called “pre-PRIMAVERA” experiments) following no specific common protocol. The impact of improved physics, on the other hand, is the subject of ongoing work in WP3, and advances have been reported in milestone MS7 (*Deliver recommendation and model configuration with improved physics for Stream 2 of the core integrations*) and deliverable D3.1 (*Quantification of robustness of aerosol-radiation-cloud interactions across models and resolution*). Here, an additional effort is aimed at quantifying the relative importance of enhanced model resolution as compared to the use of improved model physics. In order to address this challenge, a minimum experimental set is required where a given model configuration is run at i) its standard resolution (LR), ii) an enhanced horizontal resolution configuration (HR), using the same physical parameterizations as in the standard version, and iii) an “improved physics” configuration of the model run at standard resolution (LRIP). The cross-comparison between i) and ii) (impact of resolution) and between i) and iii) (impact of improved physical parameterizations) allows us to address the scientific question targeted by D2.3 in a single-model framework. Optionally, the LR, LRIP and HR triplet can be further expanded to include a fourth experiment consisting in iv) a high-resolution configuration with improved physics (HRIP). The latter makes possible to account for any possible non-linear interplay between spatial resolution and improved physical parameterization (i.e., does the efficacy of a given physical scheme improvement depend on model resolution?). Table 3.1.1 provides a sketch of the typical experimental setup adopted for the analyses presented in this report.

EXPERIMENT	DESCRIPTION
LR	Standard model configuration (standard resolution, standard physics)
LRIP	Standard resolution (as in LR) but including improved physics
HR	Enhanced model resolution, standard physics
HRIP	Enhanced model resolution (as HR) but including improved physics

Table 3.1.1. Experimental setup adopted for the assessments presented in sections 3.2 to 3.5.

Concerning the type of simulations employed for testing the relative roles of resolution and IP, no specific protocol (as for Stream 1) has been followed, given the testing purpose of the experiments, each one conducted in a single-model framework. Also, while for most of the analysed cases coupled GCMs have been used, there is a limited set of analyses for which uncoupled (forced) configurations have been employed. While the experiments performed using uncoupled configurations do not allow the establishment of a direct impact of the applied changes (either in resolution or model physics) on the simulated climate (for which a coupled integration is needed) their outcomes still hold valuable indications that might guide future developments of climate models.

It is worth mentioning that most of the participating groups performed their experimental set by testing one specific physical parameterization affecting a single component of the climate system (e.g., ocean mixing, sea-ice rheology, river routing scheme, cloud-aerosol

interaction, etc.), based on their respective field of expertise and in a single-model environment. Thus, the picture resulting from this assessment will necessarily reflect the inherent diversity in research foci featured by the PRIMAVERA partnership. In addition to the IP-dimension, the effect of stochastic physics (hereafter, SP) as compared to resolution is also addressed in this report. The decision of including analyses focusing on the relative impact of model resolution versus SP was motivated by the growing evidence supporting the use of SP as a valuable alternative route to improve climate models, compared to changes in the physics complexity.

The outline of this section essentially replicates the WP3 structure, with each specific section grouping contributions targeting processes occurring in the ocean (3.2), sea-ice (3.3), atmosphere (3.4) and land (3.5). Contributions addressing the relative impact of SP versus resolution are presented in section 3.6.

3.2 Ocean

3.2.1 Impact of upper ocean mixing and resolution: the IDEMIX and TKE schemes (MPI-M)

In order to determine possible impacts of either increased horizontal resolution or improved physics on the MPI ocean model of the North Atlantic, the Nordic seas, and the Arctic Ocean, we performed a sensitivity experiment with the MPI-ESM1.2 by either improving the horizontal resolution or the vertical mixing scheme in the ocean.

The experiment consists of four 80 year-long control simulations forced by 1950s conditions. The reference simulation is the MPI-ESM1.2-HR (Müller et al., 2018; Mauritsen et al., 2019), with a T127 atmosphere and a 0.4° tri-polar ocean grid (TP04). It uses the default Philander and Pakanowski (1981) vertical mixing scheme, so that we abbreviate this simulation as HR-PP. The first sensitivity experiment (MPI-ESM1.2-ER) replaces the TP04 ocean grid by an eddy resolving 0.1° grid (TP6M), and is referred to as ER-PP (Gutjahr et al., 2018). It uses the same configuration as HR-PP (except for changes related to a smaller time step) and the same T127 atmosphere and also the same PP scheme for vertical mixing.

The third and fourth sensitivity simulations belong to a twin experiment, where we replace the vertical mixing scheme in MPI-ESM1.2-HR. In the first we replace the PP scheme by a closure based on a prognostic equation for the turbulent kinetic energy (TKE) (Gaspar et al., 1990; Blanke and Delecluse, 1993), so that we refer to this simulation as HR-TKE. The TKE scheme is a state-of-the-art vertical mixing scheme, often used as an alternative to the K-profile (KPP) scheme (Large et al., 1994). Energy sources for small-scale turbulence are surface wind stress, buoyancy forcing and vertical shear of velocity. The only energy sink is the dissipation of TKE. Below the mixed layer, however, the main energy source in the interior ocean constitutes the breaking or dissipation of internal waves. The breaking of internal waves is usually not resolved in an ocean general circulation model but simply parameterized as a constant background diffusivity. However, this treatment creates artificial energy loss and is thus not realistic. That is where our fourth sensitivity simulation becomes useful. As with the energy budget for TKE, we introduce a prognostic energy budget for internal wave energy (IWE) by implementing the Internal Wave Dissipation, Energy and Mixing (IDEMIX) model (Olbers and Eden, 2013); we refer to this simulation as HR-IDE. We have implemented IDEMIX and TKE schemes into the Community Ocean Vertical Mixing (CVMix) Project library (Griffies et al., 2013), which we then coupled to MPI-ESM1.2. Energy sources for IWE are fluctuating wind stress at the surface that generate near-inertial gravity waves leaving the mixed layer, scattering of barotropic tides at rough topography, dissipation of mesoscale eddies or the geostrophic adjustment of large-scale disturbances. Here, we

only consider the first two energy sources and neglect the others. In the IDEMIX model the internal waves can propagate vertically and horizontally, so that they dissipate away from their source regions. The internal waves can be described as a wave continuum with an almost universal Garrett-Munk (GM) spectrum. Thus energy is transferred to smaller wave numbers and at the high-end of the spectrum energy is converted into small-scale turbulence. In other words, the dissipation of internal waves constitutes another source term for TKE. This parameterization now replaces the constant background diffusivity. In this way no artificial energy is created and the vertical mixing scheme is consistent. However, we note that in particular the dissipation of eddies is neglected, but might play an important role as a source term for IWE and TKE (Pollmann et al., 2017). In particular in the western boundary currents, such as the Gulf Stream and the North Atlantic Current, but also in the Antarctic Circumpolar Current and in the Agulhas Current, the TKE might be thus underestimated by IDEMIX without including the eddy dissipation (Pollmann et al., 2017).

Although we parameterize eddy energy and thus its dissipation (Eden and Greatbatch, 2008) in MPI-ESM1.2, we currently neither feed the dissipation of eddies into IWE nor TKE, in part because it is not well understood how and where eddies dissipate. These latter two experiments (HR-TKE and HR-IDE) allow us to (1) analyse the impact of an improved mixing scheme in the ocean, and (2) determine the explicit role of breaking internal waves. By comparing all four simulations, we can attribute changes either to improvements of the horizontal resolution or the vertical mixing.

Our first comparison is the long-standing cold bias in the North Atlantic Sea Surface Temperature, SST (Fig. 3.2.1.1). In our reference simulation (HR-PP, Fig. 3.2.1.1a), the cold bias is roughly -7.5°C in the centre at 45°N and 40°W . In contrast, a warm bias of 1°C to 3°C is simulated in the subpolar North Atlantic just south of the ice edge and in the Labrador Sea. This bias might indicate that too large a fraction of warm Atlantic Water is flowing around the boundaries of the subpolar gyre without experiencing sufficient cooling from the atmosphere. This is possibly related to the rather coarse T127 atmosphere, which underestimates for instance cold air outbreaks near the ice edge. An improvement is achieved by using a T255 resolution (see Fig.5e in Gutjahr et al. (2018)). An eddy-resolving ocean (Fig. 3.2.1.1b) reduces the cold bias in the North Atlantic noticeably, although not affecting the warm bias (this also uses the T127 atmosphere). Although the TKE scheme reduces the cold bias a little (Fig. 3.2.1.1c), it is the extension with IDEMIX that reduces the bias significantly (Fig. 3.2.1.1d); almost as much as with an eddy-resolving ocean. Using both an eddy-resolving ocean and the improved vertical mixing with IDEMIX reduces further the atmospheric cold-bias over the North Atlantic (not shown).

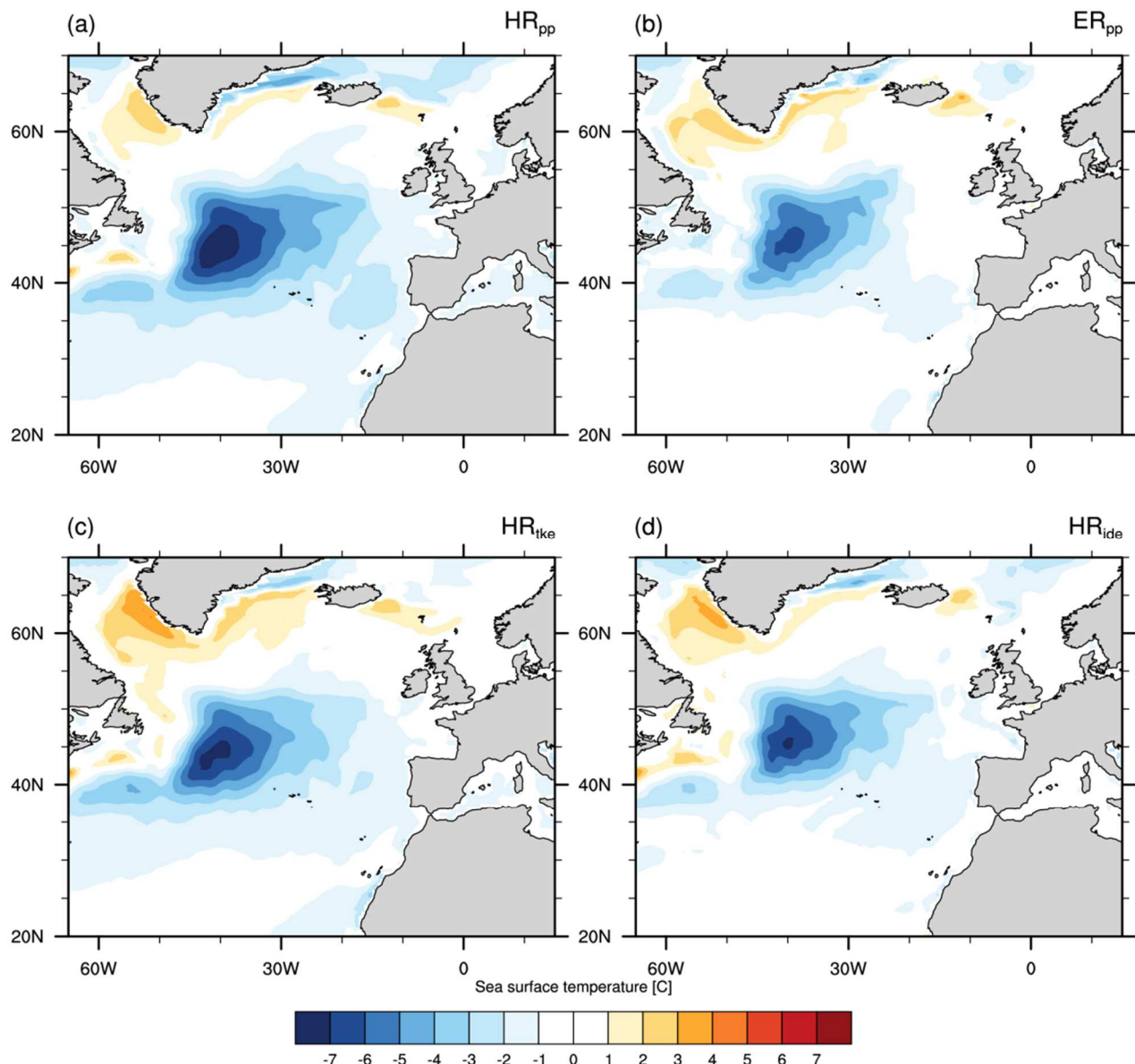


Figure 3.2.1.1. Sea surface temperature bias in the North Atlantic averaged over 50 model years with respect to EN4 (1945-1955) for (a) HR-PP, (b) ER-PP, (c) HR-TKE, and (d) HR-IDE.

The zonally averaged temperature bias (Fig. 3.2.1.2) confirms that the improved mixing scheme in HR-IDE (Fig. 2d) reduces the bias also at deeper levels, and is fairly comparable to the improvements of an eddy resolving ocean (Fig. 3.2.1.2b).

A possible explanation for this reduced warm bias in HR-IDE is increased mixing above topography due to the dissipation of internal wave energy (Fig. 3.2.1.3). For instance, the mixing is enhanced on both flanks of the Reykjanes Ridge (55°N) and above the Mid-Atlantic Ridge (35°N), where internal waves propagate upwards and dissipate in the interior of the ocean. The associated mixing changes the water properties in the North Atlantic and reduces its density and stratification.

A section along 60°N through the Labrador and Irminger Sea (Fig. 3.2.1.4) show these changes in water mass properties. In particular, the water masses are less saline in both basins in HR-IDE, so that the density reduces (Fig. 3.2.1.4d). Furthermore, the overflow waters through the Denmark Strait and over the Iceland-Faroe-Scotland ridge become less dense, because of weaker salt advection into the Nordic Seas, so that the deep water masses which form there (and drive the overflow waters) also become less dense.

On the other hand, the eddy-resolving ocean simulates less mixing at upper and intermediate depths in the North Atlantic (Fig. 3.2.1.3b) with respect to our reference simulation. This reduced mixing might be explained by reduced numerical mixing because of the finer grid (Wang et al., 2018). Thus, the reduction of the cold bias is related to a stronger North Atlantic Current, advecting more heat and salt into the subpolar gyre. As a consequence, the water masses in the Irminger and Labrador Seas are denser and more stratified (Fig. 3.2.1.4b) compared to HR-PP (Fig. 3.2.1.4a). Besides the changes in water mass properties, we see an improvement in the circulation in ER-PP. In general, the boundary currents become stronger and are better resolved, showing small-scale features, for instance the recirculation of the Irminger Gyre (IG; Våge et al., 2011) (Fig. 3.2.1.4b). This gyre causes the isopycnals to dome towards the surface in its centre at $\sim 41^{\circ}\text{W}$, whereas in the HR simulations, the IG spans the whole Irminger Sea shifting also the centre of the doming into centre of the basin. A similar contraction of the isopycnal doming can be seen in the Labrador Sea.

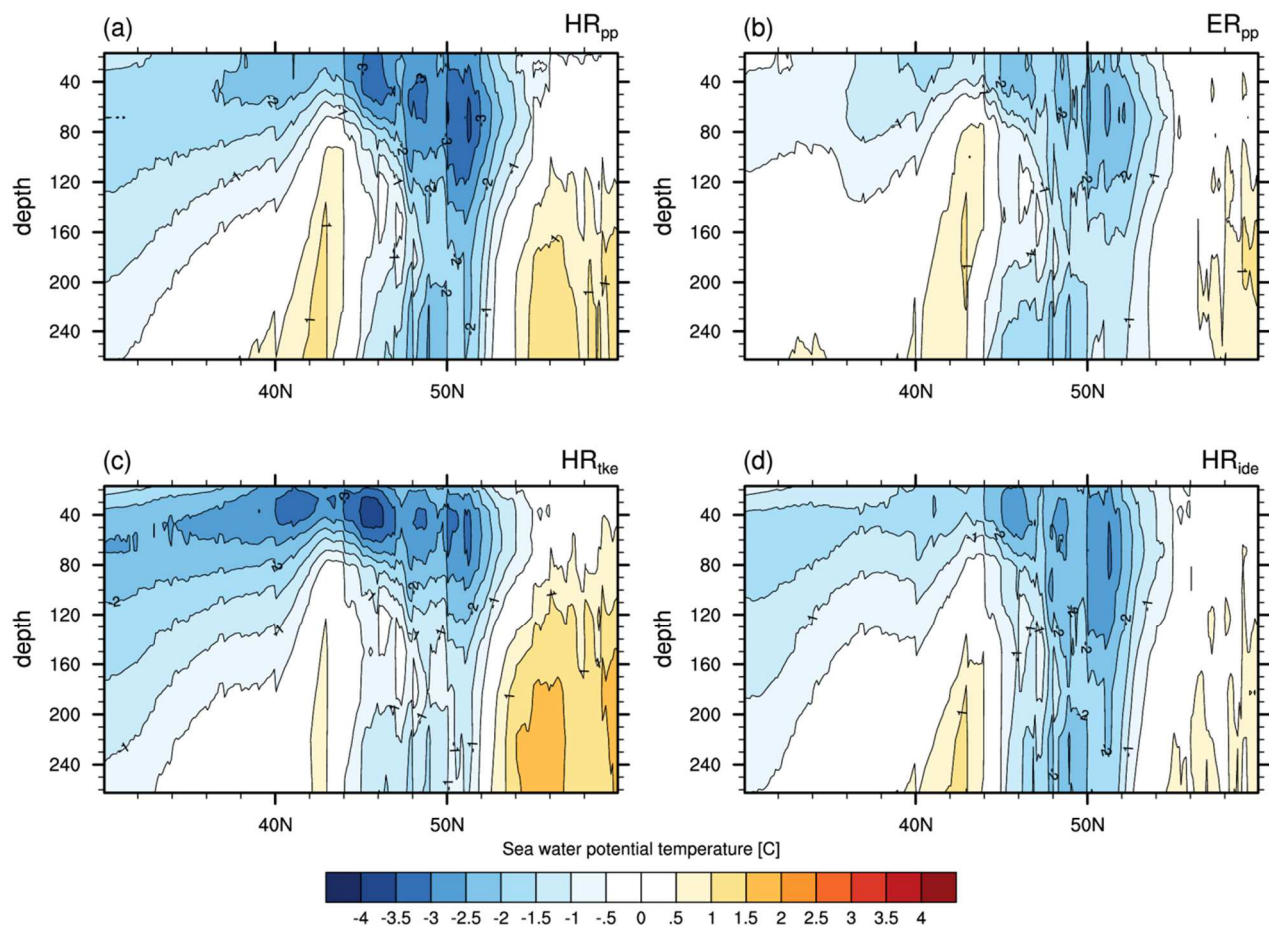


Figure 3.2.1.2. Zonally averaged temperature bias (30°N to 60°N in the North Atlantic) with respect to EN4 (1945–1955) for (a) HR-PP, (b) ER-PP, (c) HR-TKE, and (d) HR-IDE.

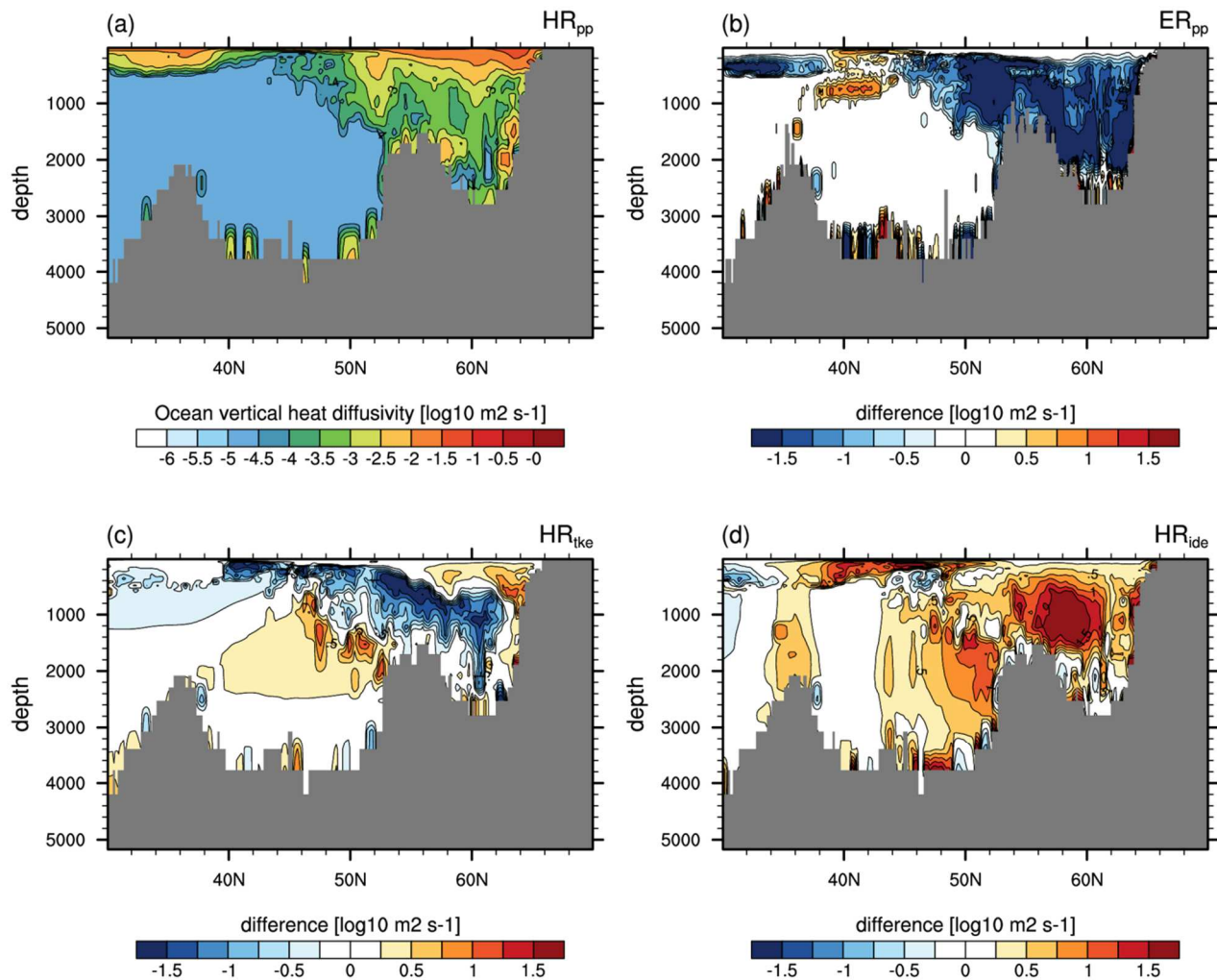


Figure 3.2.1.3. Section of diffusivity along 35°W in the North Atlantic (30°N to 75°N) for (a) HR-PP, (b) ER-PP, (c) HR-TKE, and (d) HR-IDE.

Overall, our results suggest that both an increased horizontal resolution, i.e. eddy resolving, of the ocean model and improved physics of vertical ocean mixing (IDEMIX) affect ocean quantities. However, on a global scale the eddy-resolving ocean has a larger impact (for instance on biases in the Southern Ocean, also in the atmosphere; not shown). As these are first results based on relatively short simulation periods, we cannot be confident that IDEMIX causes larger changes on a longer time scale, as possible effects on the circulation of the interior ocean take several decades to become relevant. Another aspect is that the coupled model requires retuning if the vertical mixing scheme is replaced. We decided to not retune MPI-ESM1.2 in order to see the pure effects that are introduced by the mixing scheme. However, it may happen that the model biases might become worse after such re-tuning (for instance the cold bias in the North Atlantic). On the other hand, an energetically consistent model is to be preferred compared to a simple scheme that creates spurious sources of energy.

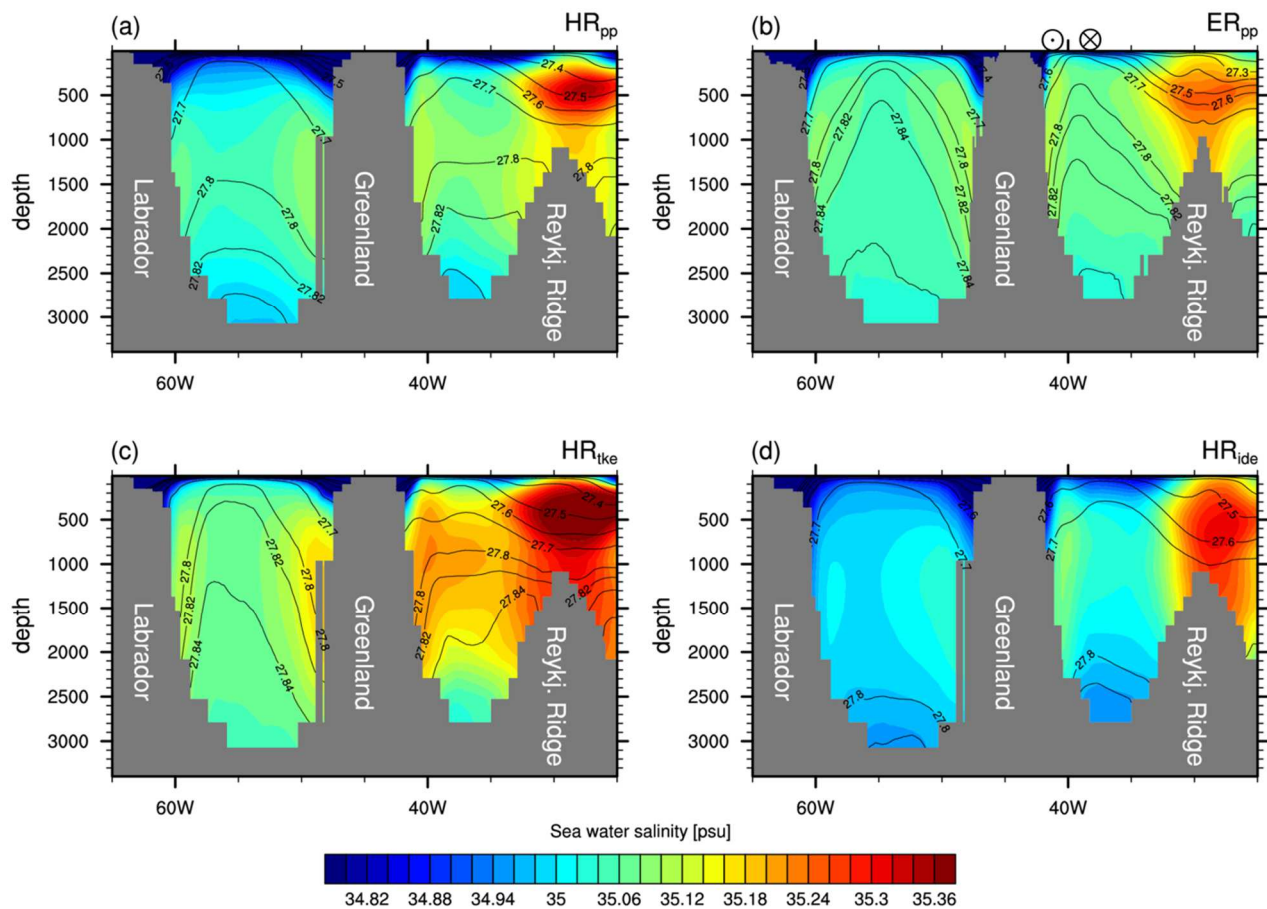


Figure 3.2.1.4. Section of salinity (colour shaded) and potential density (contours) along 60°N through the Labrador and Irminger Sea for (a) HR-PP, (b) ER-PP, (c) HR-TKE, and (d) HR-IDE. The symbols in (b) mark the southward flowing (○) branch of the East Greenland Current / East Greenland Irminger Current and the northward recirculation (⊗) closing the Irminger Gyre.

3.2.2 Impact of upper ocean mixing and resolution: the OSMOSIS scheme (NOCS)

The OSMOSIS Ocean Surface Boundary Layer (OSBL) scheme for mixing in the upper ocean is a parameterisation of Langmuir turbulence which results from an interaction between Stokes drift or shear (a residual current resulting from surface waves) and wind stress.

Comparison between observations and large eddy simulations (LES) suggest that Langmuir turbulence is present in the real-world OSBL (McWilliams et al., 1997; Thorpe, 2004). Results from LES also show that the entrainment rate associated with Langmuir turbulence is greater than that due to standard shear turbulence. Because of the increased entrainment rate, it is hoped that the parameterization of Langmuir turbulence in ocean models would reduce the shallow bias in the mixed-layer depth that is present in many ocean models, thereby potentially improving the warm bias often seen in simulations in the Southern Ocean.

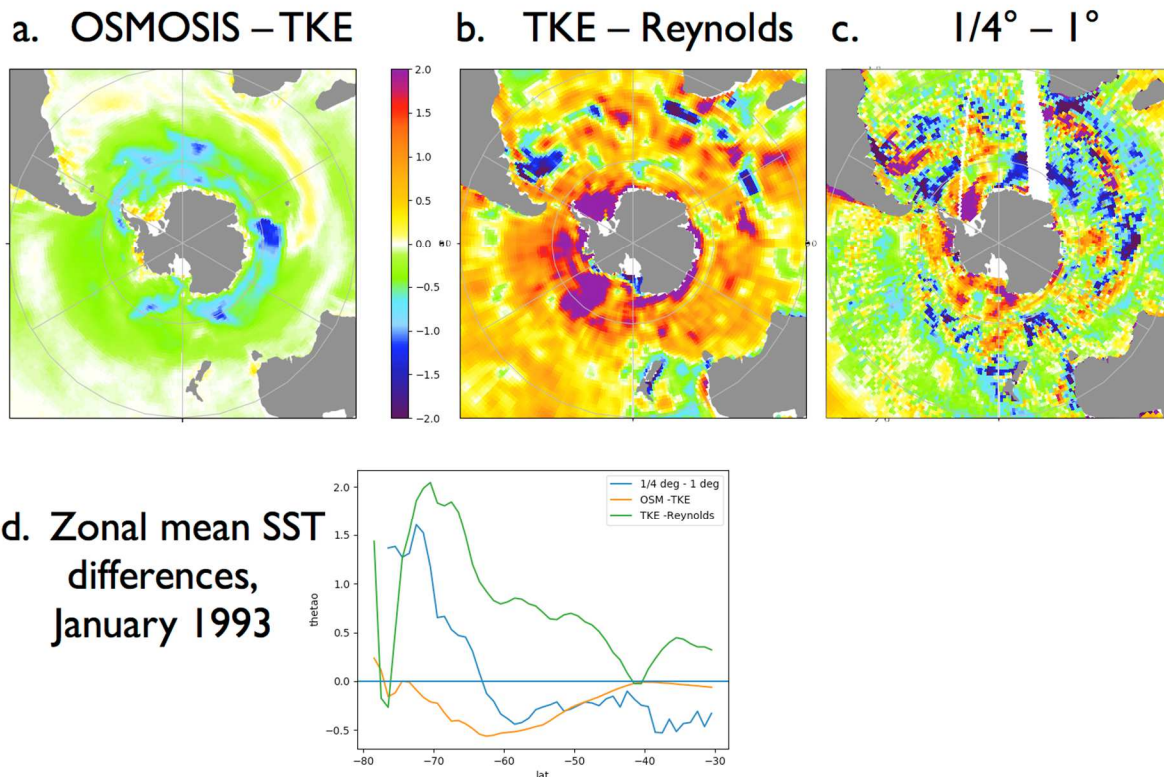


Figure 3.2.2.1. Sea surface temperature (SST) differences in January 1993 (Southern Ocean summer) for ocean models forced by interannually varying CORE-II. (a) Difference when OSMOSIS is included to represent upper ocean mixing, as compared with the standard NEMO scheme in which mixing is defined through the TKE mixing scheme. (b) Bias of 1° run of NEMO with standard TKE scheme with respect to Reynolds dataset. (c) Difference between eddy permitting 1/4° run of NEMO and 1° NEMO run, both using the TKE scheme. (d) Zonal mean differences.

The scheme parameterizes the effects of Langmuir turbulence within a 1-D model inspired by Large et al.'s (1994) K-profile parameterization (KPP) model, where diffusivities are set in terms of a depth scale (the OSBL depth) multiplied by a velocity scale and by a non-dimensional vertical profile. In the original KPP model the velocity scale is approximately proportional to the ocean-side friction velocity u^* , but lowered when the OSBL is stable (surface buoyancy input) and increased when the OSBL is unstable (surface buoyancy loss). In OSMOSIS-OSBL this velocity scale is instead based on the Langmuir turbulence velocity $u_L^* = \sqrt[3]{(u^*)^2 u_{so}}$, where u_{so} is the surface Stokes drift. A key difference is that whereas in the KPP model, the OSBL depth is set diagnostically from a Richardson number criterion, in OSMOSIS-OSBL it is instead calculated prognostically. The OSMOSIS-OSBL model also includes a careful treatment of the physics of the 'seasonal thermocline' (the region of enhanced stratification immediately below the surface mixed layer), necessitated by the prognostic calculation of the OSBL depth.

The OSMOSIS scheme has now been included in the NEMO v 4.0 trunk and is in principle available to other modelling centres in PRIMAVERA which use the NEMO ocean. This has so far only been run in ocean-only mode, in a realistic global NEMO model at 1° resolution. While improvements are evident in the summer SST biases (in the Southern Ocean), the ocean mixed layer is too deep (and cold) in the winter. This is an ongoing issue for which various solutions are being assessed, and for this reason no simulations in coupled models have so far been conducted.

The improved SST bias in the Southern Ocean summer (when the mixed layer is shallowest) is shown in Fig 3.2.2.1a above. There is an average improvement of 0.5-0.8°C between

South America/ Africa/ Australia and the Antarctic continent, where the typical warm bias of 1-2°C is seen in the standard TKE run (Fig. 3.2.2.1b) and in many other models (see below). The improvement is therefore significant.

South of about 50°S (Fig. 3.2.2.1d) the OSMOSIS improvement dominates the difference between the SST in an eddy permitting ($1/4^\circ$) resolution and in the 1° model (Fig. 3.2.2.1c), except close to Antarctica, where the eddy-permitting ocean-only model actually has a considerably worse warm bias than the 1° model. Indeed, for coupled models, the typical warm bias of 3-4°C is not much improved until an ocean resolution of $1/12^\circ$ is achieved (see Fig 3.2.2.2 below from Hewitt et al, 2016; all these models have $1/4^\circ$ ocean resolution except for (d) which has $1/12^\circ$ resolution). The warm bias for coupled models with 1° ocean resolution is similar to that shown for the $1/4^\circ$ cases.

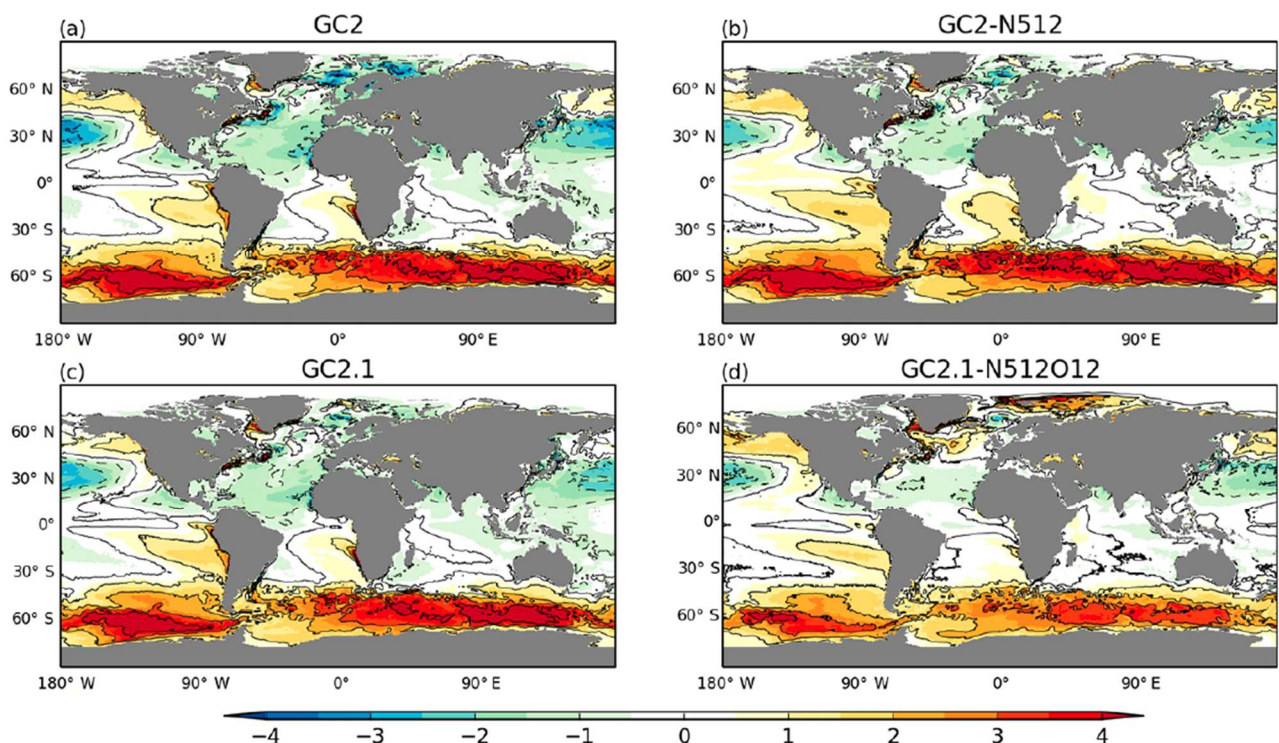


Figure 3.2.2.2. Differences between modelled SST from years 11-20 and HadISST observations in coupled models (a) GC2, (b) GC2-N512, (c) GC2.1 and (d) GC2.1-N512O12, from Hewitt et al. 2016

There is little net effect in the (northern winter) N Atlantic (not shown). In July (Fig. 3.2.2.3a and 3.2.2.3d) the OSMOSIS model produces modest cooling in the North Atlantic that tends to accentuate the cold SST bias seen in the standard NEMO TKE run (Fig. 3.2.2.3b), but ameliorates a warm bias seen in the Pacific and in the zonal mean (Fig. 3.2.2.3b and Fig. 3.2.2.3d). Increasing resolution from 1° to $1/4^\circ$, however, has a much larger impact than OSMOSIS and in the opposite sense (Fig. 3.2.2.3c and 3.2.2.3d), warming the N. Atlantic strongly.

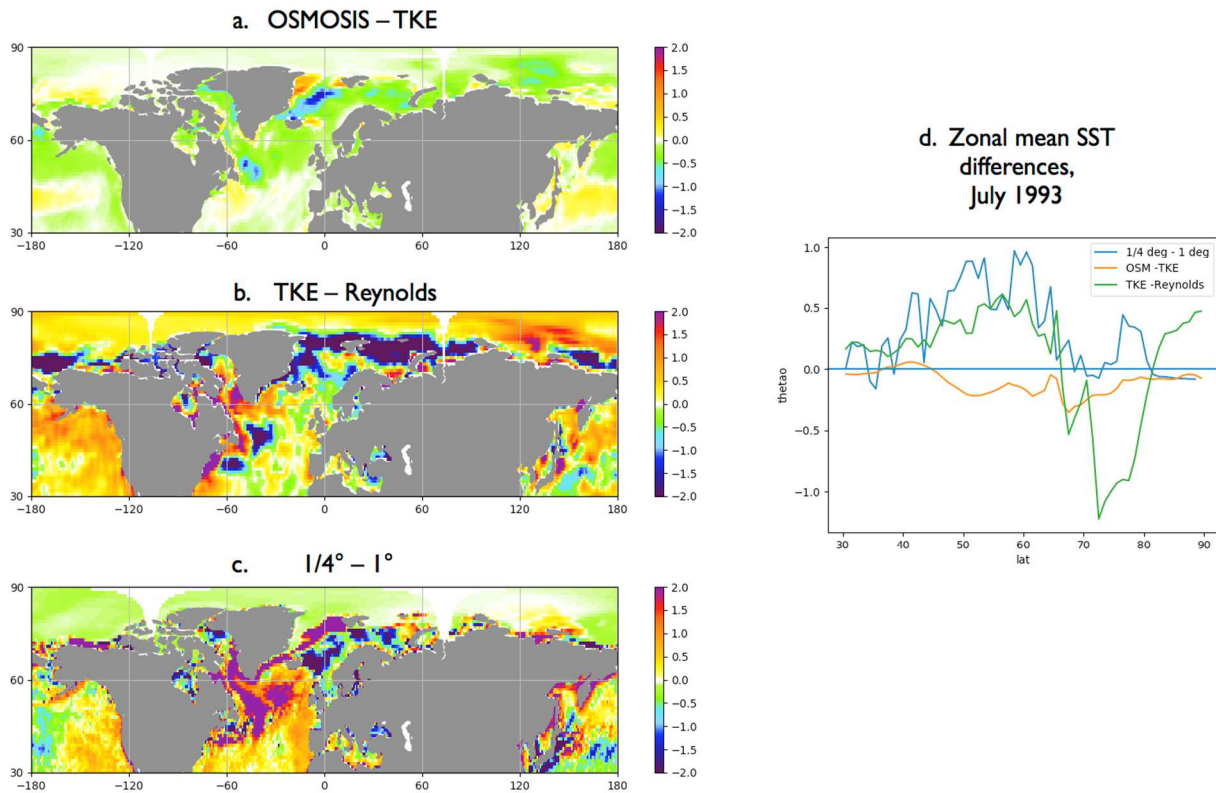


Figure 3.2.2.3. Sea surface temperature (SST) differences in July 1993 (northern summer) for models forced by interannually varying CORE-II. (a) Difference when OSMOSIS is included to represent upper ocean mixing, as compared with the standard NEMO scheme in which mixing is defined through the TKE mixing scheme.(b) Bias of 1° run of NEMO with standard TKE scheme with respect to Reynolds dataset. (c) Difference between eddy permitting $1/4^\circ$ run of NEMO and 1° NEMO run, both of which use the TKE scheme. (d) Zonal mean differences.

This strong North Atlantic warming at higher resolution (which acts to correct the cold bias in the 1° model) is also evident in the annual-mean, as shown by Marzocchi et al (2015), Fig. 3.2.2.4, which shows that the typical North Atlantic SST cold bias is by contrast much reduced (by several degrees) when the resolution is increased from 1° to $1/4^\circ$ (and further reduced at resolution of $1/12^\circ$; not shown).

In conclusion, OSMOSIS has a bigger effect in the Southern Ocean than resolution increases of 1 to $1/4^\circ$, but the opposite is true in the N Atlantic, for which increased resolution is more important. The Southern Ocean SST warm bias reduction could make a difference to the simulation of European climate through atmospheric teleconnections but this has so far not been tested (as this would need a coupled model simulation).

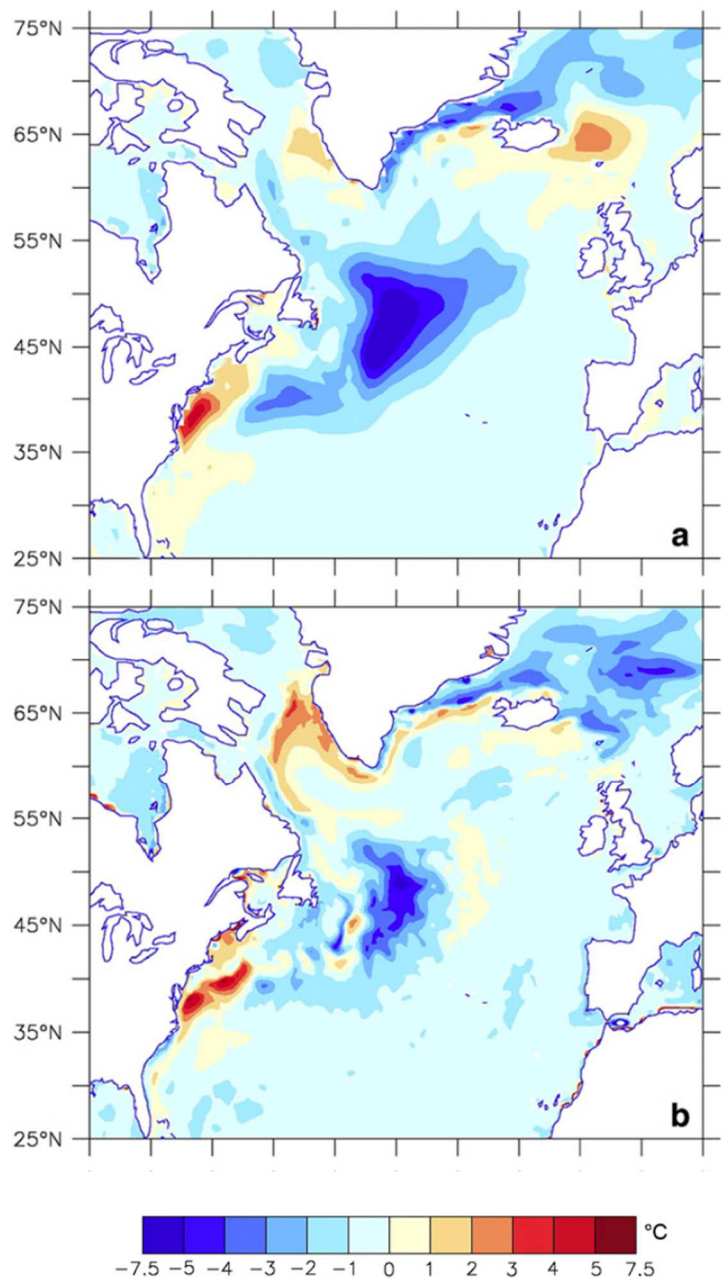


Figure 3.2.2.4. Differences between modelled annual-mean SSTs (in ocean-only forced models) and the Reynolds observational dataset in 2007 in (a) 1° NEMO and (b) $\frac{1}{4}^{\circ}$ NEMO, from Marzocchi et al. (2015)

3.3 Sea-Ice

3.3.1 Comparing the effects of melt-ponds and increased resolution in EC-Earth (SMHI)

Observations have shown that melt-ponds over the Arctic have increased. This will alter the physical and optical properties of sea ice and might even affect remote regions.

Here, we used the coupled EC-Earth3-model and performed experiments with and without melt-pond parameterization in both standard and high resolution.

We analyse the role of melt-ponds in controlling the sea ice mass and potential remote effects of melt-pond related sea ice changes, and compare these impacts to the impact of increased resolution on both Arctic and remote climate.

We performed four simulations with the coupled EC-Earth3P model for the transient period 1950-2014 following the HighResMIP-protocol:

CTRL_STD: 1950-2014 simulation with the standard-resolution EC-Earth3P (T255 in atmosphere, ORCA 1 in ocean) without melt ponds.

CTRL_HR: 1950-2014 simulation with the high-resolution EC-Earth3P (T511 in atmosphere, ORCA025 in ocean) without melt ponds.

MELT_STD (MP3_std): EC-Earth3P standard resolution including melt-ponds

MELT_HR (MP3_high): EC-Earth3P high resolution including melt-ponds

Note that the CTRL-simulations here are not the control-1950 simulations as defined in the HighResMIP-protocol.

Based on the standard and high-resolution simulations, we first analysed the impact of melt-ponds on the Arctic Sea Ice cover (SIC). Compared to corresponding standard resolution runs (CTRL_STD and MELT_STD), both high resolution simulations (CTRL_HR and MELT_HR) show a year-around reduction in the Arctic Sea Ice cover (not shown). However, the melt-pond exhibits different behaviour in standard and high-resolution simulations. This can be seen from Figure 3.3.1.1, which illustrates the temporal evolution of SIC in March and September. All simulations are characterized by similar marked natural variability at interannual and decadal timescales (Figure 3.3.1.1). We see opposite responses over certain periods between standard and high resolution simulations, which is likely due to natural variability. In order to get more detailed spatial information, Figure 3.3.1.2 shows the spatial differences between melt-pond simulations and control runs averaged over 1981-2010. It is clearly shown that the melt ponds have an opposite SIC response in high and low resolution in both March and September. While under high resolution, melt ponds lead to decreased ice concentration in the North Atlantic Arctic sector in March, ice concentration is increased in the low resolution simulations with melt ponds. In September, melt-pond leads to more wide spread responses in the Central Arctic; a reduction of SIC in low resolution and a slight increase in high resolution. Our analysis shows also that increasing resolution leads to strong Arctic sea ice reduction. However, the impact of the melt-pond scheme is still ambiguous. Meanwhile, the large internal variability of the Arctic climate system may also play an important role.

Arctic Sea Ice Area in March

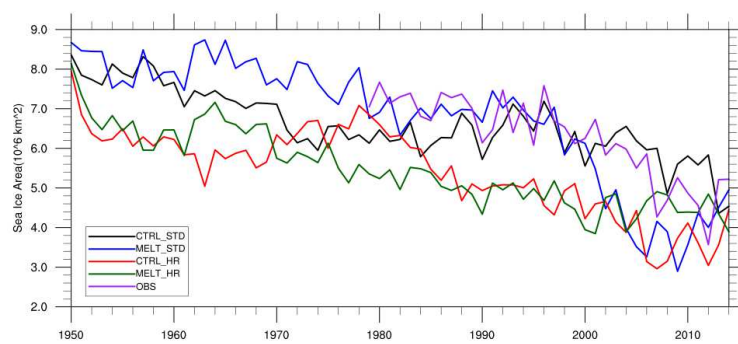
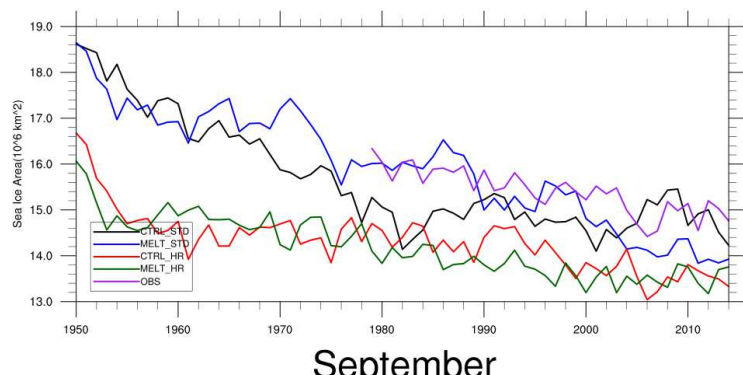


Figure 3.3.1.1. Arctic Sea Ice extent in March (top) and September (bottom) during 1950-2014 in the standard and high-resolution simulations with and without melt-ponds in EC-Earth.

Sea Ice Concentration(%) 1981-2010

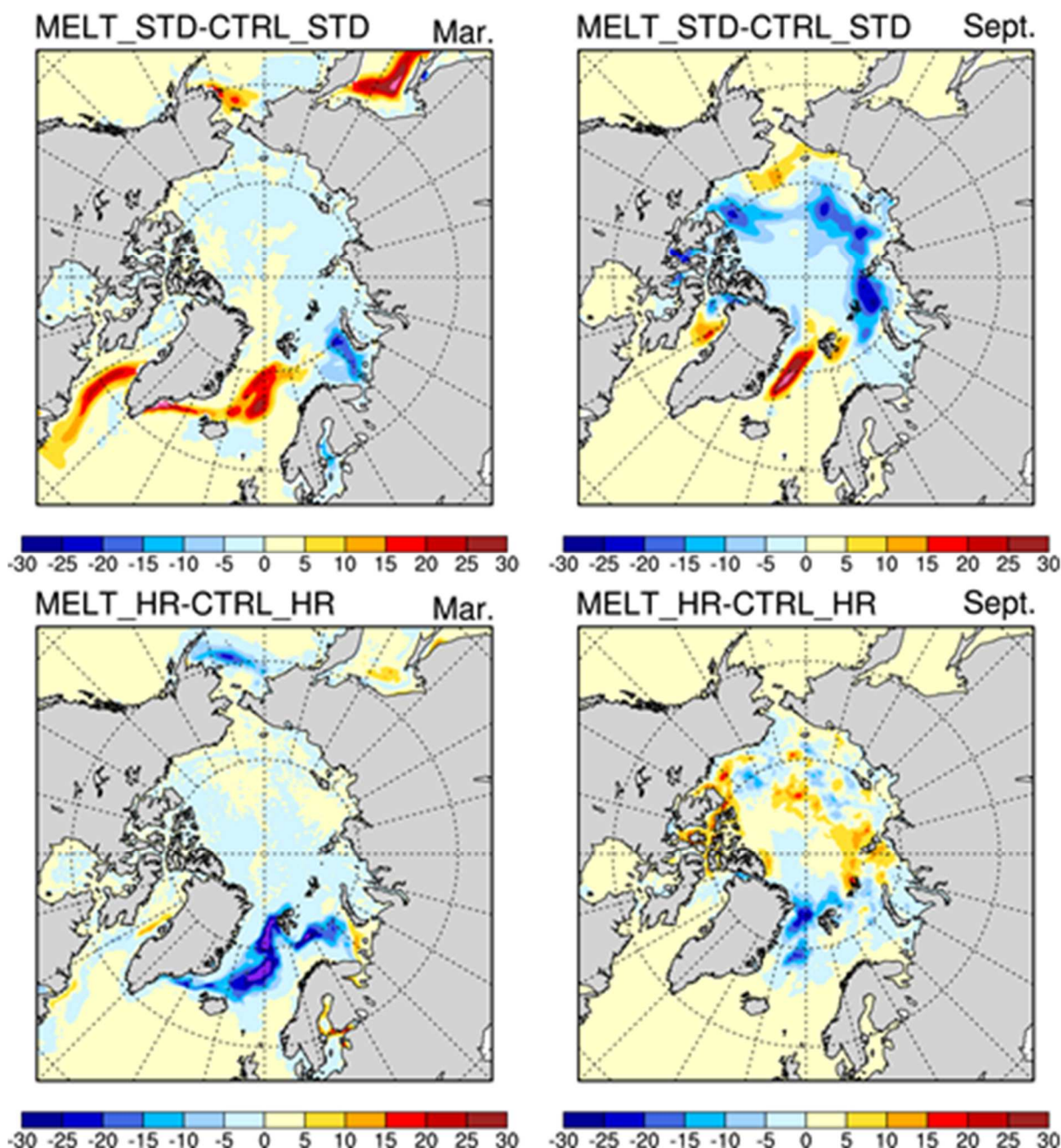


Figure 3.3.1.2. Arctic sea ice concentration differences between melt-pond simulation and control runs in March (left column) and September (right column) averaged over 1981-2010 for standard (top) and high (bottom) resolutions, respectively.

The sea ice response to increased resolution and melt-ponds leads to a pronounced local temperature effect. Enhanced surface fluxes from the ocean to the atmosphere, when sea ice area is reduced, lead to a warming and vice versa. This effect is particularly pronounced in winter when ocean-atmosphere temperature gradients are largest (Figure 3.3.1.3). In Barents, Greenland and Bering Seas, the winter time temperature response to melt-ponds and to increased resolution is of similar amplitude. In the Barents Sea, both increased resolution and melt-ponds lead to reduced sea ice and increased temperature, which reduces the cold bias in CTRL_STD in this region. In the Greenland and Bering Seas, the temperature response to melt-ponds depends on the resolution. While we see a temperature

increase (and thus a reduction of the bias) in MELT_HR in both Greenland and Bering Sea, we see additional cooling in MELT_STD.

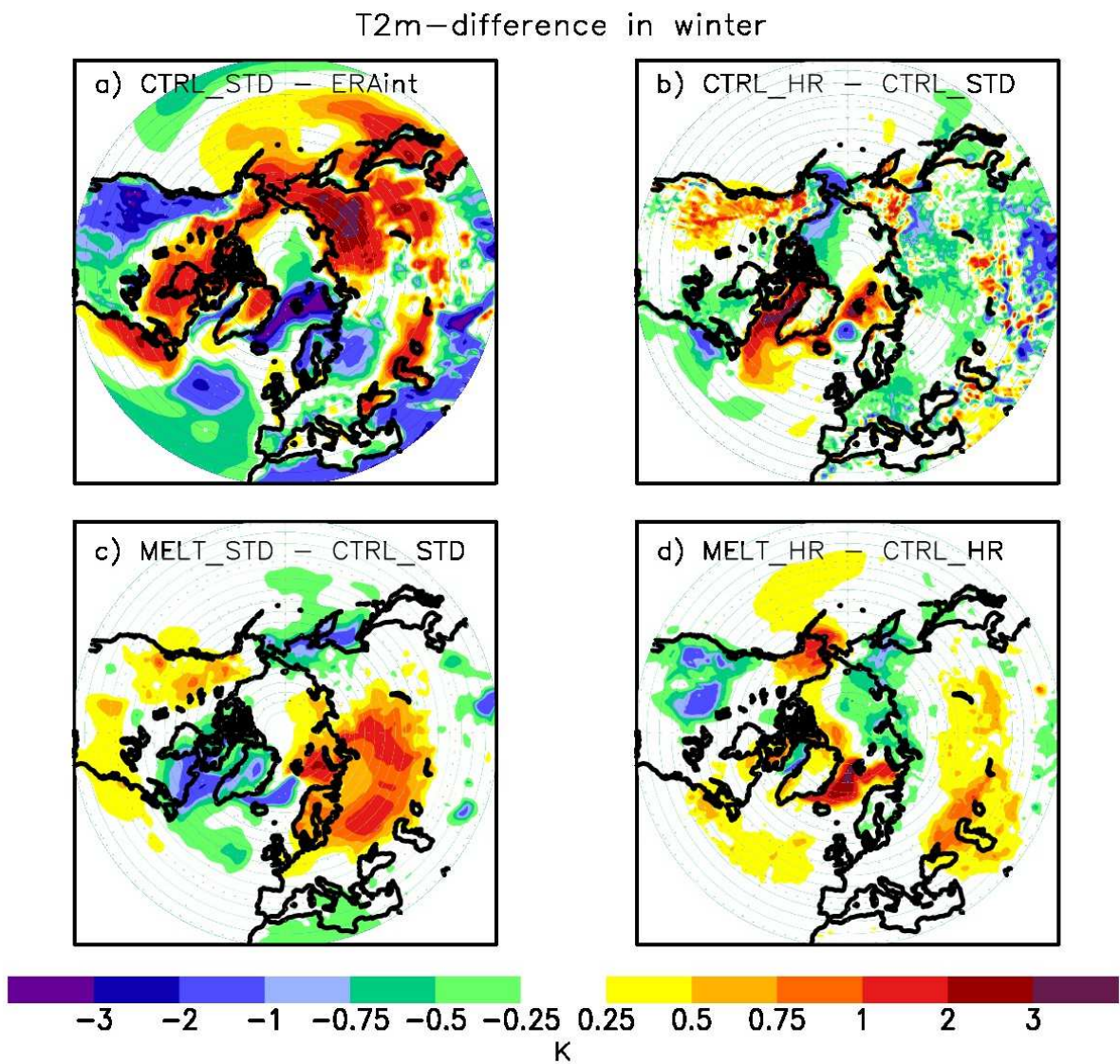


Figure 3.3.1.3. Winter differences of two meter air temperature (T2m), averaged over 1980-2014: a) CTRL_STD – ERAint, b) CTRL_HR – CTRL_STD, c) MELT_STD – CTRL_STD, d) MELT_HR – CTRL_HR. In a) and b), the values have been divided by 2.

The remote effect of melt-ponds on mid-latitude temperature also depends on the resolution. For north-eastern Europe, implementation of melt ponds leads to a winter warming and a reduction of the cold bias in this region in standard resolution. In high resolution, we see a warming over south-eastern Europe leading to an increased warm temperature bias.

Increasing resolution leads to a more widespread response with somewhat stronger temperature signals compared to the effect of melt ponds. As for the melt-ponds, it depends on the region, if this signal leads to decreased or increased temperature biases. Along the east coast of the USA and Canada, high resolution causes a cooling, which reduced the warm bias in this region and which is due to a more realistic position of the Gulf Stream in CTRL_HR (not shown).

Implementation of melt-ponds and related sea ice changes and surface heat fluxes might affect even lower latitudes by affecting the large scale atmospheric and oceanic circulations. However, our results indicate that the remote impact of melt-ponds on lower latitudes is very

small. The signal due to increased resolution is substantially larger than the effect of melt-ponds in lower latitudes (not shown).

Generally, the results for the other three seasons agree with winter: in mid and higher latitudes, the effects of melt ponds and increased resolution are of similar amplitude while in lower latitudes, the impact of melt-ponds is small.

The melt-pond implementation seems to lead to some systematically different responses depending on the resolution. In MELT_HR, a warming in the Nordic Seas and in the Atlantic Arctic Sector occurs in all seasons. In MELT_STD, we see instead a warming from the Barents Sea eastwards along the Siberian coast and mostly colder temperatures compared to CTRL_STD in the Canadian Archipelago, Baffin Bay and partly also in the Greenland Sea.

To conclude, the implementation of melt-ponds into EC-Earth leads to a slight reduction of sea ice area and volume in the Arctic. This effect is more pronounced in low resolution than in high resolution.

Locally, the temperature response to melt-ponds is of similar amplitude as the impact of increasing resolution.

In lower latitudes, temperature and circulation responses to increased resolution are substantially larger than the impact of melt-ponds.

The changes caused by both melt ponds and increased resolution can, depending on the region, increase or decrease biases in the standard model version of EC-Earth. Locally, we found systematic reductions of the biases, e.g.: both melt-ponds and high resolution lead to improved sea ice concentration in the Barents Sea and reduced cold biases in EC-Earth; a better position of the Gulf Stream in the high resolution simulations improves the warm biases along the east coast of North America.

The large natural variability complicates the interpretation of the results and might contribute to the different responses of ice, temperature and circulation to melt ponds and increased resolution. To make more robust statements on the potential effect of melt ponds on the atmospheric circulation and lower latitude climate, ensembles of simulations with and without melt ponds would be necessary. Thus, this study also contributed to the recommendation to perform additional ensemble members as part of the PRIMAVERA-Stream 2 simulations.

3.3.2 Comparison of improved physics (sea-ice categories) and resolution on Arctic sea ice (BSC)

We first compare the impact of changing model resolution and physical parameters on the representation of Arctic sea ice in coupled simulations performed with EC-Earth. In the figures below, we compare the standard resolution (T255-ORCA1) stream 1 simulation (blue), the standard resolution stream 2 simulation (purple) and the high resolution (T511-ORCA25) stream 1 simulation. The stream 1 standard resolution experiment had important problems in the North Atlantic (AMOC too weak, sea ice too far south) and for that reason, the stream 2 simulation was produced by modifying three ocean-model parameters:

- Decrease in the TKE penetration below the mixed layer
- Increase in the Langmuir cells coefficient
- Increase in thermal conductivity of snow

Comparing the two stream 1 simulations shows the impact of increasing the model resolution, which can then be contrasted with the impact of simply changing a small subset of model parameters (comparing stream 1 and stream 2 at standard resolution). The focus is

here on the Arctic sea ice. Figure 3.3.2.1a shows the seasonal cycle and Figure 3.3.2.1b shows the time series of monthly averages of Sea Ice Extent (SIE) for the months of September (yearly minimum) and March (yearly maximum). In addition, Figure 3.3.2.1c,d illustrates the differences in the integrated Ice Edge Error (IIEE), defined as the area where the model and the observations disagree on the ice concentration being above or below 15%, that is, the sum of all areas where the local sea ice extent is overestimated or underestimated (Goessling et al. 2016). This metric is more reliable than the SIE to evaluate the realism of the model in representing the sea ice cover, as by definition it integrates all errors, while in the second case, errors of different sign can compensate one another. The IIEE can be additionally decomposed in two errors with complementary information: the Absolute Extent Error (that represents the absolute difference in the simulated and observed sea ice extent) and the Misplacement Error (which happens when the models fails to represent the sea ice in the right location).

From Figure 3.3.2.1a we noticed that increasing the resolution (blue vs red) leads to an increase in sea ice cover in the Arctic, an effect that seems to be present year round, but particularly prominent in winter. Whether SIE is underestimated or overestimated in these simulations is strongly dependent on the observational dataset used for validation (and the time of the year). Unfortunately, this leads to some ambiguity as to whether the sea ice cover improves with resolution: the high-resolution simulation is closer to OSISAF (EUMETSAT SAF, 2016) while the low-resolution simulation is closer to NSIDC (Cavalieri et al., 1996). This is further evidenced by comparing the IIEE in 3.3.2.1c and 3.3.2.1d. When OSISAF is used as a reference (Fig. 3.3.2.1c), we note a reduction in the IIEE, an improvement which comes from a substantial reduction in the AEE (dashed line) in the high resolution simulation. Using NSIDC (Fig. 3.3.2.1d) leads to the opposite conclusion.

On the other hand, changing the physical parameters (blue vs magenta) lead to a general reduction in sea ice cover, and this is accompanied with a reduction in IIEE, in particular during winter where the stream 2 simulation shows smaller values than the stream 1 simulation. Interestingly, decomposing the IIEE shows that the changes in physical parameters introduce a massive improvement in the misplacement error, while leading to a worsening of the AEE. The long-term decline of sea ice is qualitatively captured by all simulations, although it is generally underestimated in the boreal summer compared to observations. It is worth noting that the changes detected here, in particular those linked to the increase in resolution, do not apply to the Antarctic region (not shown).

We can compare these changes with the impact of changing sea ice thickness distribution (ITD). The ITD defines the fraction of area covered by ice in a particular thickness range. In the NEMO-LIM3.6 ocean–sea-ice model, the ITD is discretized into a fixed number of categories (5 by default). When this number is modified, both the position and the resolution of the thickness categories vary following the default LIM discretization algorithm, which increases the ITD resolution for the thinnest ice. We perform a series of 18 sensitivity experiments in which the number of categories is varied between 1 and 40. These experiments are run using the ORCA1 resolution and are forced by the DRAKKAR Forcing Set version 5.2 (DFS5.2; Dussin et al., 2016). The impact of varying the ITD is relatively small for the period 1979–2014 and both the mean SIE seasonal cycle and the maximum and minimum SIE temporal evolution are very similar across different ITDs (Fig 3.3.2.2a,b). By contrast, the ice volume steadily increases with the number of categories in all seasons as a result of a net enhancement of basal ice growth rates (Massonnet et al., under review); above 3 categories, the simulated ice volume quickly diverges from reanalysis estimates (*ibid*). The impact on the IIEE and its components by the different ITD is also small (Fig. 3.3.2.2c). Note that the IIEE is smaller in these simulations than in the HR and LR coupled simulations, which might be explained by the different model setup: whereas the HR and LR are free-coupled atmosphere–ocean simulations, the ones with different ITD are forced by an atmospheric observational reanalysis, which imposes a strong constraint to the model

sea ice extent based on observations. In this case, the results for Antarctica are similar as those of the Arctic. We plan to run a similar analysis when introducing a new melt pond scheme in LIM, but these results are not available yet.

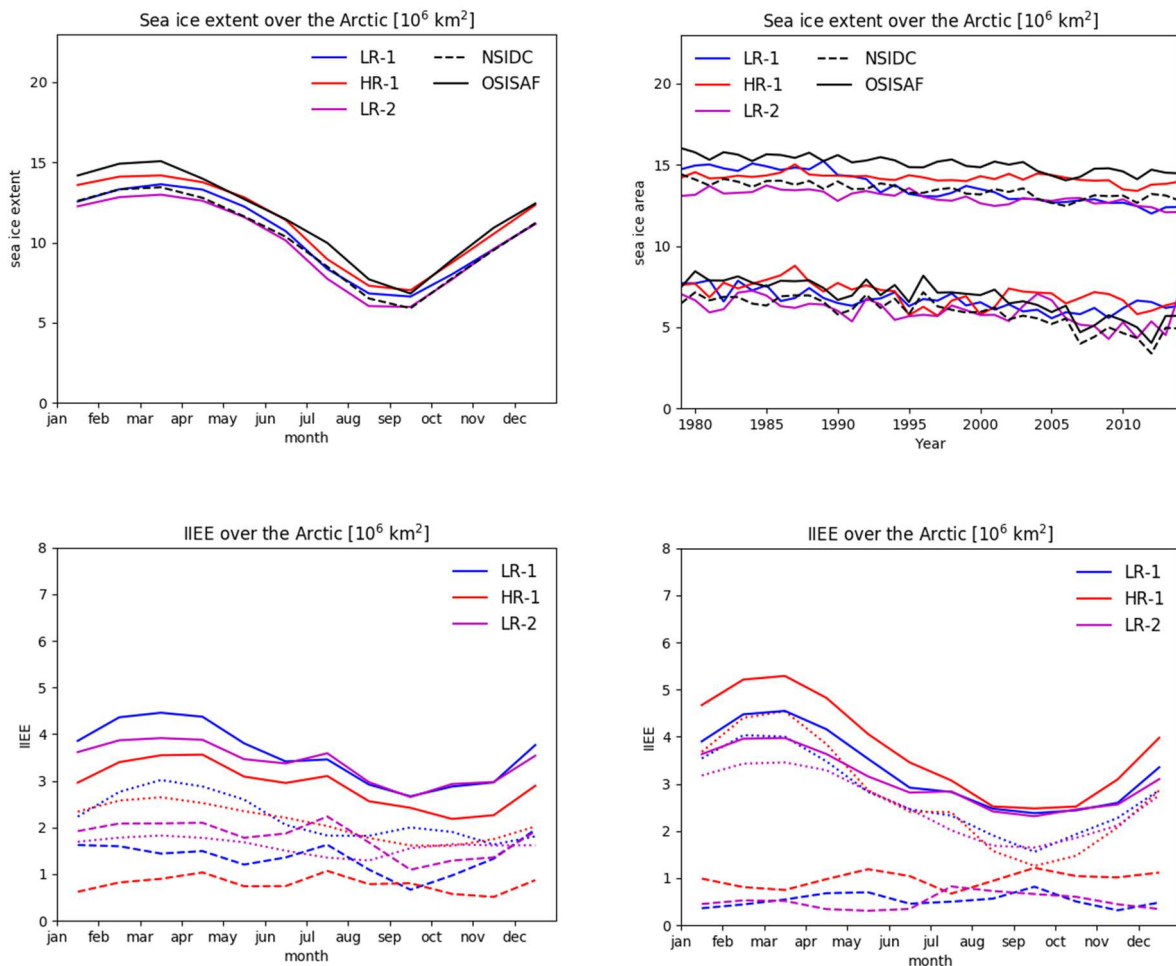


Figure 3.3.2.1. (a) Seasonal change in integrated sea ice extent for the 1979-2014 climatology, (b) interannual change in integrated sea ice extent in March (local winter) and September (local summer). The high-resolution Stream I is in red, the standard resolution Stream I in blue and the standard resolution Stream II in magenta. Sea ice concentration derived from OSISAF (NSIDC) is shown with a black (dashed) line; OSISAF. (c) Seasonal change in the integrated sea ice edge error (IIEE, solid lines), and its components, compared to OSISAF product: the absolute extent error (AEE, dashed lines) and the misplacement error (ME, dotted lines). (d) Same as (c) but when comparing with the NSIDC product. The IIEE is defined as the sum of all areas in which simulated sea ice concentration is either overestimated or underestimated compared to observations (Goessling et al., 2016).

In conclusion, changing the sea ice thickness distribution has had little impact on the sea ice extent simulated by the model, while change in ocean model parameters leads to a definite improvement in the sea ice cover. The impact of increasing model resolution on the sea ice was ambiguous in this case, as the change in sea ice cover was within the observational uncertainty.

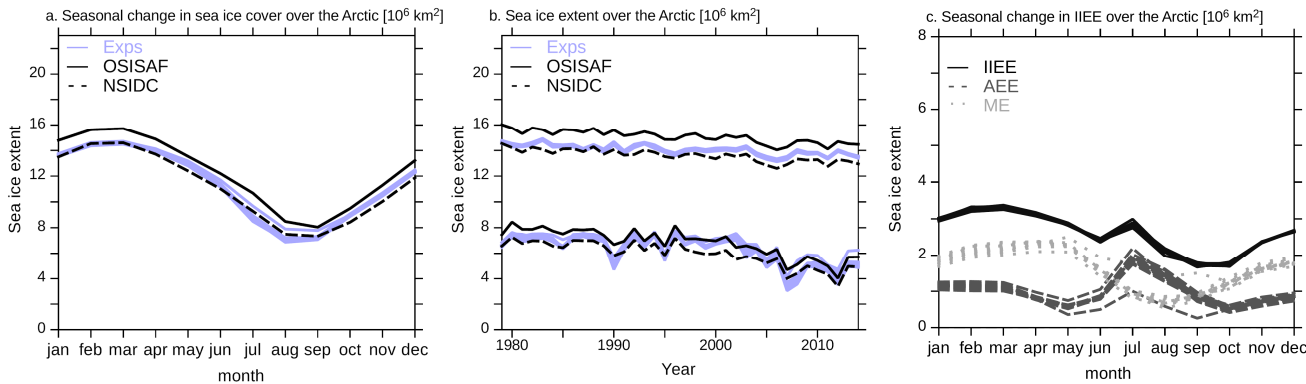


Figure 3.3.2.2. (a) Seasonal change in integrated sea ice extent for the 1979-2014 climatology, (b) interannual change in integrated sea ice extent in March (local winter) and September (local summer). Shown in both figures is the sea ice concentration in the Ocean and Sea Ice Satellite Facility on Ocean and Sea Ice observational product (black, solid line; OSISAF), the National Snow and Ice Data Center observational product (black, dashed line; NSIDC), and the simulations with different ITD (purple lines). (c) Seasonal change in the integrated sea ice edge error (IIEE, solid lines), and its components, the absolute extent error (AEE, dashed lines) and the misplacement error (ME, dotted lines), with respect to OSISAF.

3.3.3 Impact of resolution and sea-ice physics complexity on Arctic sea ice and European climate (ECMWF)

To differentiate between the impact of model resolution and improved physics schemes in the ECMWF model (Roberts et al., 2018) we compare the Stream 1 simulations (performed at different resolutions) with a set of experiments performed with different sea ice model physics. We consider the impact on the mean state for Arctic sea ice variables and also for European climate variables (2m temperature, mean sea level pressure (MSLP) and precipitation) for the region defined as the $35\text{-}70^\circ\text{N}, 15^\circ\text{W}\text{-}40^\circ\text{E}$. We show that the increased ocean resolution tends to bring model mean state closer to the reanalysis state over the European region, both in terms of the annual mean and the seasonal averages. In general the mixed resolution of high resolution ocean and low resolution atmosphere performs better than when the highest resolution atmosphere is used. Changes in the model physics can bring about changes in mean state that are comparable with resolution changes in terms of Arctic variables, but over Europe an impact is only seen in the MSLP in certain seasons. Preliminary results suggest that there is a comparable impact of sea ice model physics and resolution on the wintertime North Atlantic Oscillation. This aspect needs to be investigated further.

a) Experimental Description.

To consider the impact of resolution and changes in model physics on the simulated European climate a series of coupled model integrations is examined. More details are within Table 3.3.3.1.

To determine the impact of resolution we make changes to the ocean and atmospheric horizontal resolution and run the model from 1950 to 2014 (for details see Roberts et al. 2018 and the description of Stream 1 hist-1950 integrations). All these model runs were made with an atmospheric component model IFS CY43R1 with 91 vertical levels and an ocean component model NEMO3.4, LIM2 with 75 vertical levels.

To determine the impact of model physics changes we use only the mixed resolution of low resolution atmosphere and high resolution ocean for further testing. The atmosphere and ocean models are upgraded, by using later model versions, that is CY45R1 for the

atmospheric component and NEMO version 3.6 for the ocean (which is not used operationally by ECMWF). The ice model physics was also improved by moving from LIM2 to LIM3. The main differences in LIM2 and LIM3 is its prognostic variables and formulation of the ice rheology. LIM3 has prognostic salinity rather than using a constant value and models the ice thickness distribution, rather than parameterising it. LIM3 uses an EVP rheology rather than the VP formulation used in LIM2. We further test the impact of ice thickness distribution by running LIM3 with 1 and 5 categories. As analysed initial conditions did not exist for LIM3, we used a forced ocean-ice run to provide an initial state for 1980 for the ocean-ice model. Coupled integrations were then performed for 1980-2014.

Results shown here are for the common 30 year period of 1984-2014 for all integrations.

Experiment name	Atmosphere model	Atmosphere resolution	Ocean-Ice model	Ocean resolution	Ice physics model	Rheology
LR-LIM2	IFS CY43R1	Tco199 (~50km)	NEMO 3.4	1°	LIM2 (1 cat)	VP
MR-LIM2	IFS CY43R1	Tco199 (~50km)	NEMO 3.4	0.25°	LIM2 (1 cat)	VP
HR-LIM2	IFS CY43R1	Tco399 (~25km)	NEMO 3.4	0.25°	LIM2 (1 cat)	VP
MR-LIM2	IFS CY45R1	Tco199 (~50km)	NEMO 3.6	0.25°	LIM2 (1 cat)	VP
MR-LIM3-1C	IFS CY45R1	Tco199 (~50km)	NEMO 3.6	0.25°	LIM3 (1 cat)	EVP
MR-LIM3-5C	IFS CY45R1	Tco199 (~50km)	NEMO 3.6	0.25°	LIM3 (5 cat)	EVP

Table 3.3.3.1. List of coupled model configurations used. We highlight the differences between the models in terms of resolution and model version which defines the physics schemes used.

b) Impact on Arctic Mean State.

Figure 3.3.3.1 shows a summary of the model mean (1980-2014) sea ice extent and volume for different seasons along with the mean state of the ocean reanalysis product ORAS5 (Zuo et al. 2018). First we consider the impact of resolution (compare the differences in filled circles). Figure 3.3.3.1 shows that the mean sea ice state of the low resolution model is the furthest from the reanalysis mean state. Increasing ocean resolution from low resolution (1 degree) (purple filled circle) to high resolution (0.25 degree) (orange filled circle) has a big impact on the mean state of the ice. The additional increase in atmospheric resolution from (50km to 25km) (blue filled circle) does not show a clear improvement in mean state. Improvements are seen in extent for spring and summer but not in volume.

The impact of changing model physics in both the ocean and atmosphere can be seen by comparing the open and filled orange circles. We see that in this case the sea ice mean state is further from the reanalysis than the original version. This highlights the importance of model setup alongside resolution changes. The impact on model bias can be as large as changing the resolution; this could be down to a variety of reasons, such as the removal of a compensating error or different parameter values in the model setup. For example parameter settings in the atmosphere are focussed on operational forecast resolutions around 10km rather than the 50km resolution that these climate runs were carried out at. It should be noted that the Stream 1 experiments use a model version which has been used operationally and has had the parameter values tuned within uncertainty ranges to give the best model climate for short to seasonal range coupled forecasts. For the sea ice experiments at mixed resolution a default setting was used.

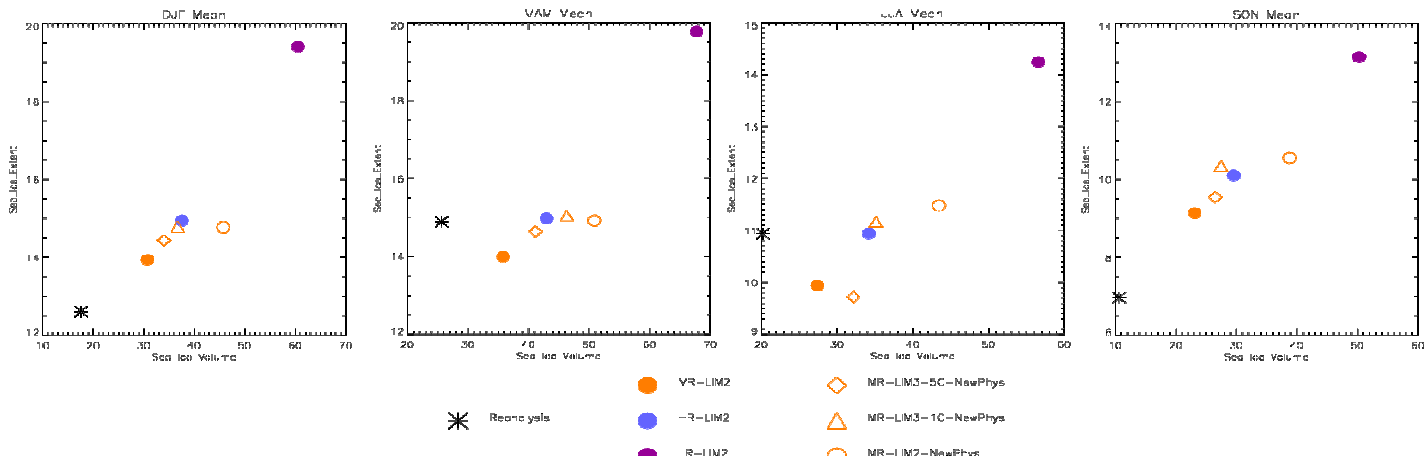


Figure 3.3.3.1. Seasonal mean fields for 1984-2014. Sea ice volume against sea ice extent for different coupled model experiments. Filled circles show stream 1 experiments with varying resolution: low resolution ocean and atmosphere (purple); high resolution atmosphere and ocean (blue); mixed resolution, low resolution atmosphere and high resolution ocean (orange). Open shapes show different model physics at mixed resolution (orange): LIM2-1 category (circle); LIM3-1 category (triangle) and LIM3-5 categories (diamond). Reanalysis values for the same period shown with a black star.

Improving the model sea ice physics brings the mean state closer to the reanalysis and modelling the ice thickness distribution improves things further. LIM3-5C consistently produces lower ice volumes and extents on all seasons. There is still a positive bias in volume. The models tend to produce a sea ice extent that is too large except in summer, where the multi-category LIM3 and the mixed resolution LIM2, have negative bias in sea ice extent. Although the sea ice biases are reduced when moving to improved sea ice physics the mean state is not always better than the LIM2-MR version.

c) European impact.

We wish to determine the relative impact of changes on European climate. Figure 3.3.3.2 shows the scatter plot for mean two-meter (2m) temperature and precipitation. In terms of temperature and precipitation there is a clustering of the runs with different sea ice model physics, revealing a marginal impact of sea ice physics on the mean state. This highlights that there is not a strong control mechanism in these coupled models between sea ice representation and mean model state over Europe in terms of temperature and precipitation. There is an impact on the precipitation and 2m temperature which is generally improved by increasing ocean resolution. We see little difference between the models run with a high resolution ocean in terms of MSLP bias (not shown). The biggest impact on European mean state bias is the resolution.

There is, however, a difference in European MSLP pressure biases in the winter and spring with different sea ice volume. This is seen when we change resolution and model physics. More analysis is needed to understand this. Winter and spring is when we expect the largest impact on large scale flow to happen when the ocean can provide significant heat exchange with the atmosphere if the sea ice is thin or not present.

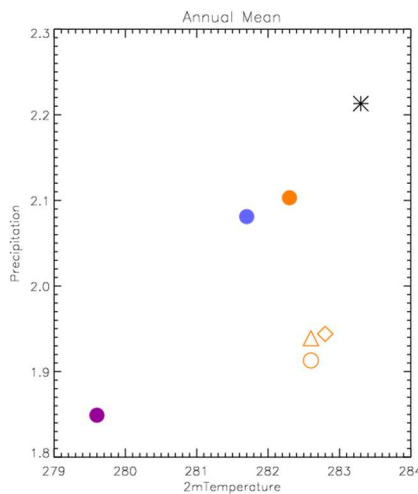


Figure 3.3.3.2: As for Figure 3.3.3.1 but for annual mean 2m Temperature (K) and precipitation rate (mm/day) over the European region for reanalysis and the different coupled model runs.

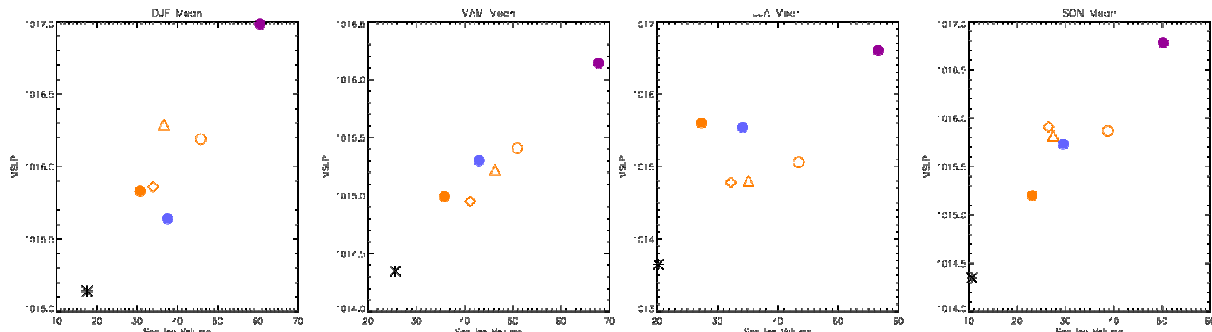


Figure 3.3.3.3. As in Figure 3.3.3.1 but for mean Arctic sea ice volume against mean European mean sea level pressure for winter, spring, summer and autumn.

d) Impact on internal variability.

In terms of interannual prediction for the European regions one of the key elements is the ability of models to reproduce the internal modes of variability. The dominant mode is the North Atlantic Oscillation (NAO) in winter. The leading empirical orthogonal function (EOF) for mean sea level pressure from reanalysis (ERA5 Hersbach et al. 2018) is used here to define the NAO; it explains about half of the atmospheric variability in winter. The pressure pattern also impacts the temperature and precipitation fields associated with the NAO. In its positive phase (as shown in Figure 3.3.3.4) it leads to warm wet winters in northern Europe and in its negative phase to cold and dry winters. The modelled NAO, can be sensitive to model biases both in the atmosphere and ocean (Keeley et al. 2012). Preliminary analysis here shows that the change in resolution and sea ice physics can have a similar sized impact the pattern (strength of the pressure dipole and associated jet) as well as fraction of variance explained.

The impact of upgraded atmosphere and ocean components tends to improve the NAO representation in the model, although pressure gradient is too high. Improving sea ice physics from single category to multi-category improves the NAO pattern and dipole strength.

EOF1 of Mean Sea Level Pressure (hPa) DJF 1985-2010

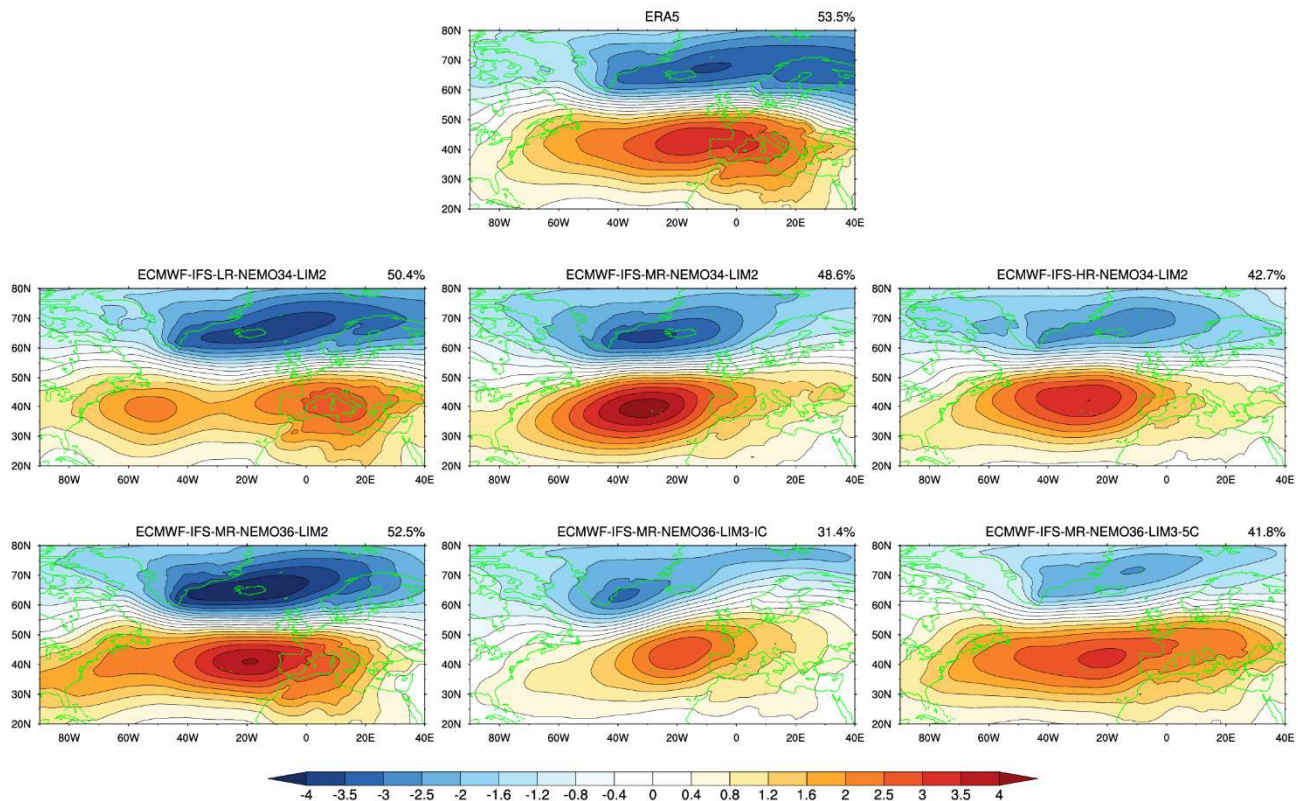


Figure 3.3.3.4. Leading mode of variability (EOF1) for MSLP for North Atlantic - European region.

3.4 Atmosphere

3.4.1 The representation of simulated Arctic rainfall/snowfall as a function of model physics and resolution (KNMI)

The Arctic is the region where the climate is very sensitive to enhanced greenhouse forcing; observations show that the Arctic warms 2-3 faster than other parts of the globe (Holden, 2012, pp. 102-103). At the same time, the uncertainty in Arctic warming is very large, because the climate processes responsible for increasing temperatures are still quite uncertain. One of the mechanisms that is not well known relates to the changed hydrology, and more specifically, to the increase in Arctic precipitation and its link to the strong warming (Bintanja & Selten, 2014).

Here we focus on Arctic precipitation and its dependence on temperature. While recent research has shown that Arctic precipitation will strongly increase with future warming, it is often assumed this increased precipitation will fall in the form of snow (Liu, Curry, Wang, Song, & Horton, 2012). Very recently, it was found that the Arctic will experience considerably more rainfall when the climate warms (Bintanja & Andy, 2017). This change in Arctic precipitation type will have a strong impact on the Arctic hydrology, climatology, ecosystems and economy (Berghuijs, Woods, & Hrachowitz, 2014) (Screen & Simmonds, 2012). This is because the form in which the increased precipitation will fall (snow or rain) is a crucial factor for the extent, magnitude and potential irreversibility of the impacts. Moreover, the effects will not be confined to the Arctic region, because changes in ocean density and sea ice will potentially impact the global climate.

The climate variables that are considered here are: snowfall, total precipitation and temperature. These variables are analysed using three model configurations: EC-Earth 2.3 (old version), EC-Earth-3P (PRIMAVERA version) and EC-Earth 3P-HR (PRIMAVERA version at high resolution). Note that EC-Earth 2.3 and 3P have a similar resolution). We use JRA-55 reanalysis data as "observations" because the Arctic is largely devoid of actual observations (mainly due to the remote location and the harsh conditions). Obviously, reanalysis data are not actual observations, but they represent the best observation-like data for the Arctic. After careful consideration, it was decided to use the JRA-55 reanalysis as 'observations', because JRA seems to best represent the snowfall fraction in the Arctic (Bintanja & Andy, 2017).

EC-Earth 2.3 uses a very simple diagnostic scheme to distinguish rainfall and snowfall, based on the ambient temperature. EC-Earth-3P is the most recent EC-Earth version with updates in cloud scheme and precipitation components compared to EC-Earth 2.3. In the new version 3.2, precipitation types are resolved prognostically, including several types of solid precipitation (see Forbes and Tompkins, 2016, for details). Hence, in terms of simulating rainfall/snowfall, version 3P represents a significant improvement in terms of the physics involved. This analysis will investigate whether these model changes will lead to a better representation of rainfall/snowfall in the Arctic, and whether changes in model resolution (in the new version) will also lead to more accurate results.

Comparing all three model versions with JRA-55 for the period 1981-2010 in terms of annual mean snowfall ratio (the ratio of snowfall to total precipitation) clearly shows that the old model (version 2.3) severely underestimates the snowfall ratio over much of the Arctic Ocean (Figure 3.4.1.1). In contrast, the PRIMAVERA version (3P) simulates much higher snowfall ratios over the central Arctic, in better agreement with the "observations". Comparing normal to high resolution in the new model version results in only minute differences. From this we conclude that the update in model physics has led to a stronger improvement compared to the application of increased model resolution.

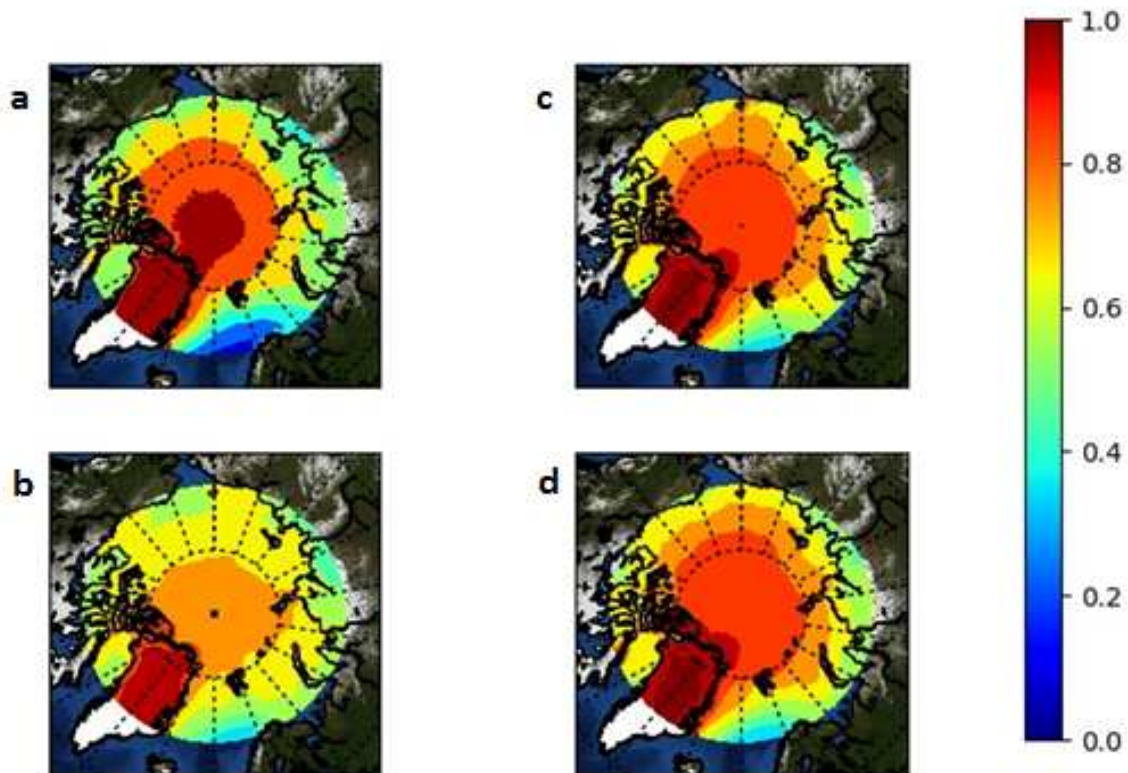


Figure 3.4.1.1. Geographical distribution of the model-mean snowfall ratio in the Arctic region for time period 1981-2010. (a) JRA ('observations'). (b) EC-Earth 2.3. (c) EC-Earth 3P. (d) EC-Earth 3P High Resolution.

A similar result is found when looking at the summer (JJA) only results (Figure 3.4.1.2). The snowfall fraction in the old model is severely underestimated, which improves in the new model, but snowfall fractions are still somewhat too low compared to JRA-55. In this case, increasing the model resolution seems to slightly increase the snowfall fraction over the low resolution model, but even in this case the snowfall fraction is underestimated in the central Arctic. The effect of model resolution on precipitation is through atmospheric dynamics, with smaller-scale systems and gradients being represented more accurately in the high resolution version (not shown).

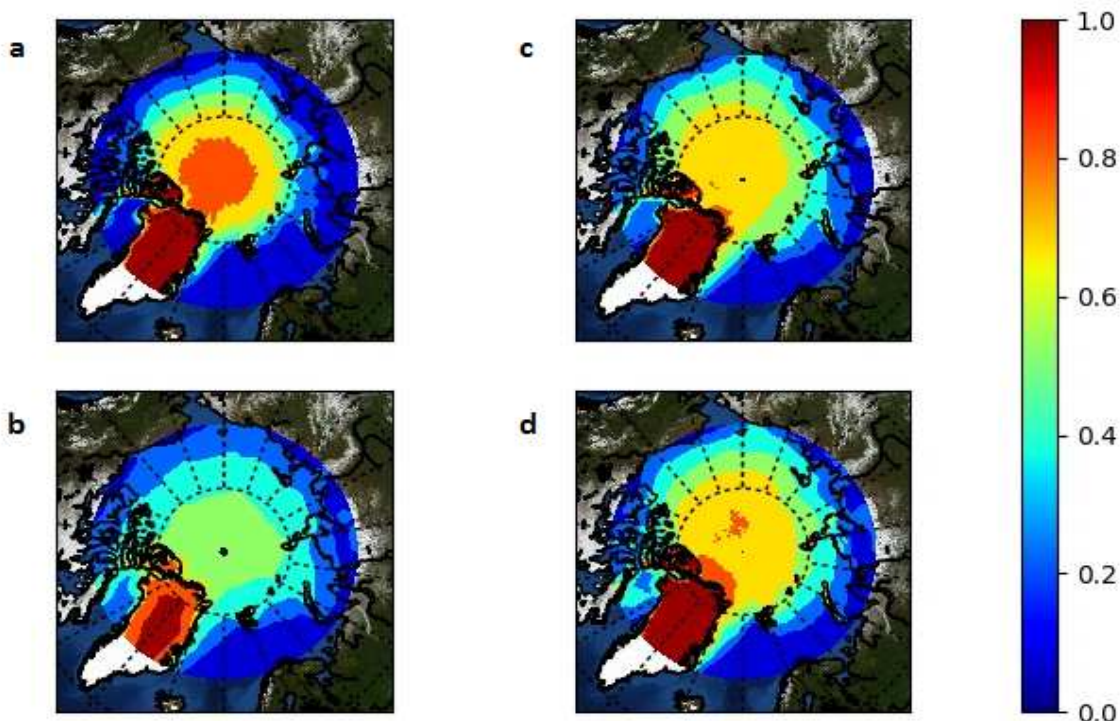


Figure 3.4.1.2. Geographical distribution of the model-mean snowfall ratio during the summer in the Arctic region for time period 1981-2010. (a) JRA ('observations'). (b) EC-Earth 2.3. (c) EC-Earth 3P. (d) EC-Earth 3P-HR.

3.4.2 The relative impacts of physics complexity and resolution on clouds, aerosols and radiation (UREAD).

PRIMAVERA Work Package 3a (WP3a) aims at quantifying the robustness of radiative fluxes, clouds, and aerosol-cloud interactions across models of different horizontal resolutions and with representations of clouds and aerosols of varying complexity. A good simulation of the coverage and water content of clouds is an important feature of a climate model because clouds strongly contribute to the radiative budget of the Earth and constitute a climate feedback mechanism. Aerosols also modify the Earth's radiative budget and are important agents of climate change because a sizeable fraction of aerosols are emitted by human activities.

Developing the cloud and aerosol schemes used by the models participating in PRIMAVERA was not part of WP3a activities but because aerosol schemes were replaced in Stream 1

simulations by direct prescriptions of optical properties and cloud droplet number concentrations, there was a need to compare against the original interactive schemes. In that context, the aim is to quantify the disadvantage of simplifying model physics because of the need to increase resolution. Simple prescriptions reproduce the radiative effects of aerosol-radiation interactions from complex models very well (see deliverable D3.1, section 3.1). In contrast, simple prescriptions of interactions between aerosol and clouds need to account for temporal variability in cloud droplet number to reproduce the radiative effects of complex models. That behaviour is consistent over most regions of the globe, including North Atlantic and Pacific Oceans and the Tropics. These conclusions support continuing the use of simplified representations of aerosols, although adding a prescription of the variance of cloud droplet number concentrations would have benefits. It is not known however whether those conclusions remain true when simulating future scenarios.

Regarding cloud water content, increasing resolution does not generally make substantial differences unless the models become very high resolution, about 7 km horizontal grid spacing. At such high resolutions, the Met Office Unified Model simulates moisture flux into extratropical cyclone clouds (storm tracks) very well compared to satellite observations, although complex cloud microphysics are required (McCoy et al., 2019). So, beyond relative merits of increased resolution or increased complexity, the answer seems to lie in a high-resolution/high-complexity combination.

Cloud radiative effects are not sensitive to resolution on a zonal average (Thomas et al. 2018). Figure 3.4.2.1 illustrates that finding by comparing absolute differences in cloud radiative effects between observations from the Clouds and Earth's Radiant Energy Systems (CERES) satellite instrument and PRIMAVERA simulations by three different grid resolutions in the Hadley Centre Global Environmental Model (HadGEM3) and two different grid resolutions in the EC-Earth3, Max Planck Institute Earth System Model (MPIESM), and ECMWF Integrated Forecast System. Although models show large differences with CERES, especially at high latitudes, those differences are not resolution dependent. In contrast, cloud radiative effects are very sensitive to model complexity, initial conditions of the simulations, and the coupling between atmosphere and ocean. Higher resolutions lead to regional improvements compared to satellite estimates of radiative fluxes in HadGEM3 in convective regions and in MPIESM in stratocumulus regions. The simulated cloud radiative effect response to the North Atlantic Oscillation does not improve systematically with increasing resolution in the PRIMAVERA models (Thomas et al. 2018).

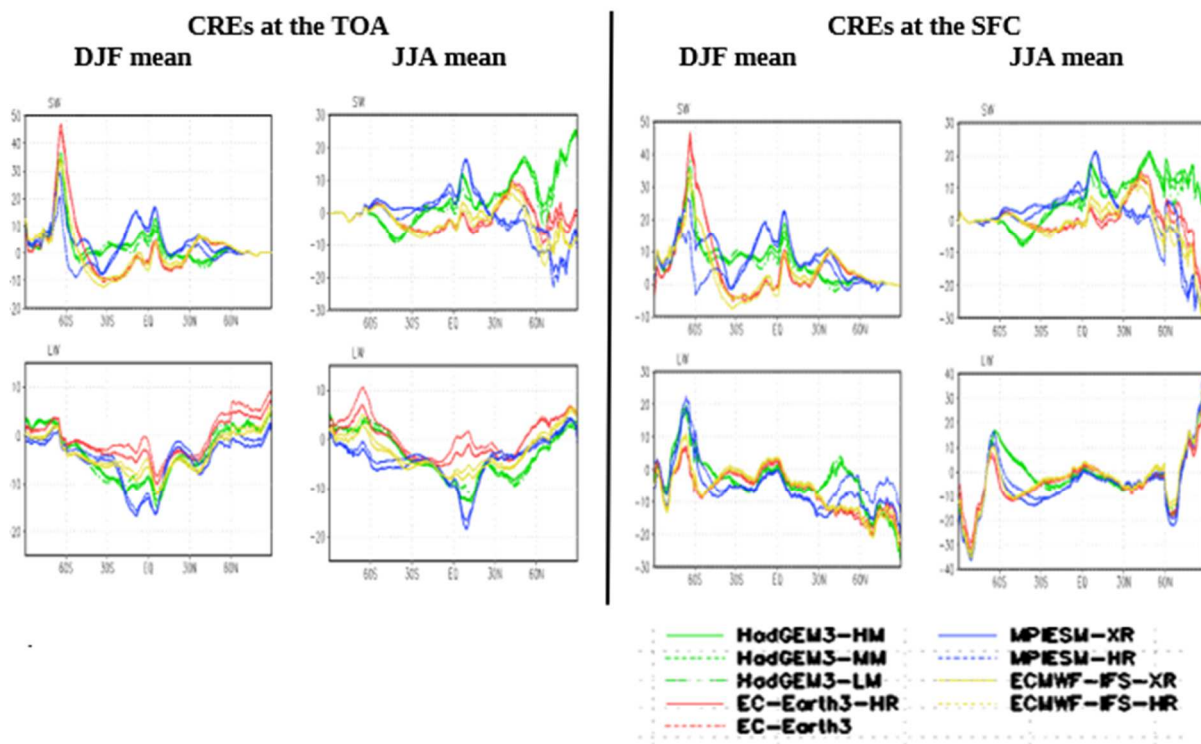


Figure 3.4.2.1. Model simulated shortwave and longwave cloud radiative effects (CRE) in W m^{-2} shown as differences from observations at (left panels) the top-of-atmosphere (TOA) and (right panels) surface (SFC) for December-January-February (DJF) mean and June-July-August (JJA) mean.

The transition between stratocumulus and cumulus cloud regimes was not found to be sensitive, on a climatological basis, to resolution or the complexity of the aerosol representations in HadGEM3. Figure 3.4.2.2 shows the vertical cross section of cloud liquid water together with the mean cloud fraction in the North East Atlantic transition for the JJA and DJF seasons. The vertical axis is logarithmic to accentuate the boundary layer cloud structure. The model captures the transition in the JJA season with the shallow and liquid boundary layer clouds in the north-eastern domain and the deep convective clouds in the southern parts. But neither the horizontal resolution nor the aerosol scheme complexity have a large impact on the representation of the clouds along the transition. There are however differences in median precipitation rate (PRIMAVERA deliverable D3.1, section 3.4). Generally, the high-resolution model version has a lower median rain rate than the low-resolution version. The aerosol representation also have an impact, with higher rain rate when aerosols are interactive rather than prescribed. The existence of changes in precipitation rates may lead to differences in future climate feedbacks.

Climatology of cloud liquid water and fraction along NEA transect

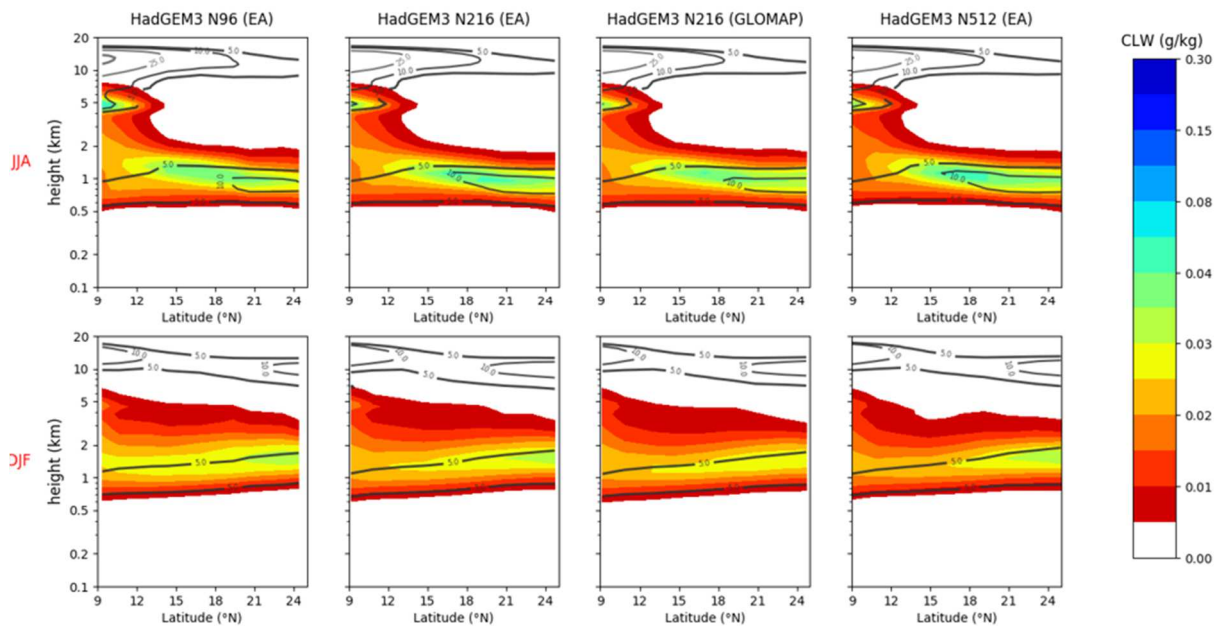


Figure 3.4.2.2. Mean vertical cross section of cloud liquid water (filled contours) and cloud fraction (contours) along the North Earth Atlantic stratocumulus-to-cumulus transition in versions of HadGEM3-CG31 at N96, N216 and N512 horizontal grid resolutions using either the fully interactive aerosol scheme GLOMAP (third column) or the simplified prescriptions EasyAerosol (EA, columns 1, 2, and 4). Upper panels show the north-hemisphere summer season (June-July-August) and lower panels show the winter season (December-January-February).

In summary, there are benefits of increasing resolution for simulating clouds, aerosols, and radiation, but those benefits may require very high resolutions to fully appear. Those benefits are also modulated by the complexity in model physics. Complex cloud microphysics help make the most of very high resolutions, at least in terms of simulating cloud water content in extratropical cyclones. Similarly, simplifying the representations of aerosol-cloud interactions offset some of the gains of increasing resolution when simulating cloud cover and albedo.

3.5 Land

3.5.1 The impact of improved soil boundary conditions and river routing scheme (UREAD, CMCC)

a) Land-surface model sensitivity to soil boundary conditions.

A new global soil mineral and organic matter map based on the Montzka et al. (2017) data set was adapted and tested on JULES and CLM land surface models (LSM), in use at UREAD and CMCC. The enhanced soil boundary dataset was tested with global land-only LSMs (JULES and CLM) simulations and compared against simulations using the conventional LSMs soil maps. Equivalent GCM simulations have also been carried out with HadGEM3, albeit not yet with CLM. The simulations were conducted for the period 1979-2012 and forced by WFDEI (Weedon et al., 2014). The soil hydraulic model in JULES is Brooks and Corey (1964), in CLM is Clapp and Hornberger (1978). The set of simulations is:

- JULES CTL: using the conventional soil boundary conditions.
- JULES NEW SOIL: using the enhanced soil maps.

- CLM CTL: using the conventional soil boundary conditions (IGBP, Global Soil Data Task, 2000).
- CLM NEW SOIL: using the enhanced soil maps.

The introduction of the novel soil boundary condition (organic matter and soil mineral maps) leads to an improved representation of the water stored in the top soil layer for both models. Figure 3.5.1.1 shows a general reduction in mean bias when models estimates are compared to observed soil moisture data (ESA CCI). In both models there is a significant reduction of biases at high latitudes of the northern hemisphere. Globally, JULES reduces the RMSE by about 16%, while CLM by about 32% suggesting a more realistic representation of the soil state with the new dataset. Further investigation is required to better evaluate the impact of the soil boundary condition on other components of the water cycle.

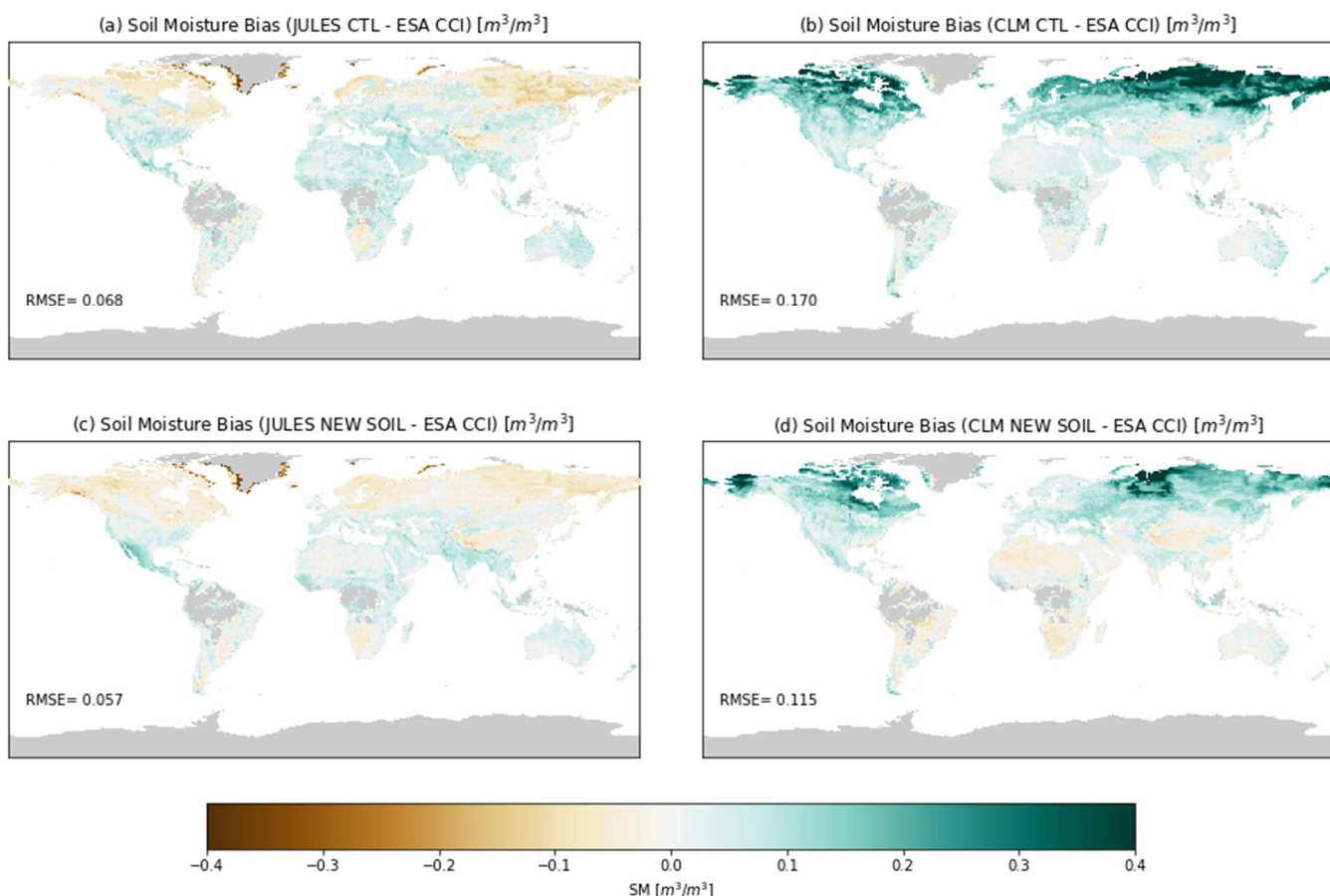


Figure 3.5.1.1. Bias map of simulated soil moisture in the top soil layer (10 cm) using ESA CCI (Dorigo et al 2017) as reference. Top panels show the biases when conventional soil boundary conditions are used in (a) JULES and (b) CLM, while bottom panels present the biases when the novel soil maps are included in both models. Grey shades indicate missing observed data. The RMSE is included in all maps.

b) Advances in river routing modelling.

Improved versions of Total Runoff Integrated Pathways (TRIP, Oki et al. 1999) and River Transport Model (RTM, Branstetter 2001) were tested on JULES and CLM respectively. For TRIP in JULES, a set of river routing auxiliary variables was adapted to enhance the rivers paths resolution from 1deg to 0.5deg. For RTM in CLM, the river velocity computation has been updated in order to account for both slope and water amount as main driver.

Enhanced versions of river routing in JULES and CLM were compared against their original versions. In JULES, the river routing is defined according to the direction of the flow and sequence (the hierarchy) of each grid-cell. An increased resolution of these variables (from 1.0deg to 0.5deg) was implemented to have a better definition of river pathways mainly on regions of complex orography. In CLM, the original river routing scheme (RTM) computes river velocity only based on slopes. RTM is improved by introducing the dependency of river velocity on water amount and on river flow. In both LSMs, the original and the new versions of their river routing schemes are tested. JULES simulations are forced by WFDEI for 1979-2012, while CLM is forced by GSWP3 for 1901-2014 as the change in RTM is appreciable in long-term. The set of simulations is:

- JULES TRIP: using the ancillary files at 1.0deg.
- JULES NEW TRIP: using the ancillary files at 0.5deg.
- CLM RTM: using the original version of RTM.
- CLM NEW RTM: using the enhanced RTM.

Figure 3.5.1.2 presents the sensitivity of LSMs to the alternative river routing schemes at catchment scale. In JULES, most basins have similar river discharge for both resolutions of TRIP, suggesting that the increased resolution does not have a high impact on the mean annual cycle of river flow. In CLM, the improved physics of RTM leads to a general improvement of the model reproduction of river discharge seasonal cycle, especially in tropical areas. This suggests so far that a more complex model, like RTM, may be required to benefit from resolution, while TRIP does not possess sufficient degrees of freedom. Further analysis will be done to assess the global impact of the improved river routing schemes.

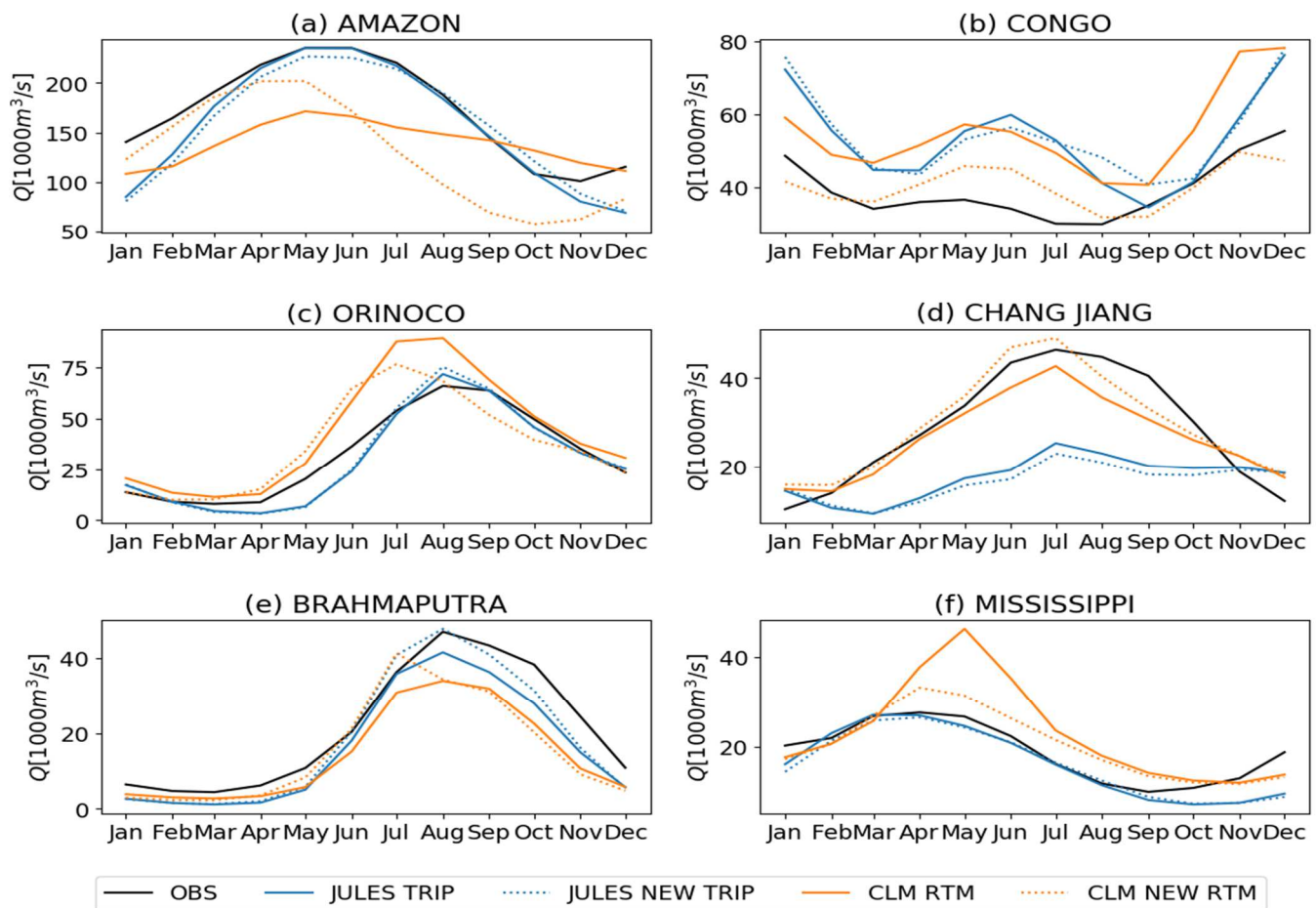


Figure 3.5.1.2. Observed and simulated river flow mean annual cycle (1979-2012) for the 6 basins with the highest discharge.

c) Sensitivity to different forcing resolutions (JULES)

Previous works in PRIMAVERA showed that high resolution GCMs overestimate land precipitation when compared with gridded observations (Vanniere et al. 2018, Roberts et al. 2018). In particular, grid point models (e.g., HadGEM) show a significant increase on regions of complex orography, where the scarcity of gauge stations increase the uncertainty of gridded observations. To assess the effect of such differences in precipitation on river discharge, a set of JULES simulations have been run turning rivers on. Six simulations forming three different ensembles were conducted. The main difference among ensembles are the forcings, while difference between members is the soil boundary conditions (with and without the novel dataset presented in Section 3.5.1.a). The ensembles are:

- WFDEI: JULES forced by WFDEI (gridded observations).
- LM: JULES forced by low resolution (N96) HadGEM 3.1 from Stream 1.
- HM: JULES forced by high resolution (N512) HadGEM 3.1 from Stream 1.

In terms of hydrograph correlation, JULES forced by gridded observations has higher performance than JULES forced by GCMs as expected. In terms of biases, the river discharge is underestimated in seven out of 10 selected basins when JULES is forced by gridded observations (see green and black boxplots in Fig. 3.5.1.3). On those basins, the supposed excess of precipitation estimated by HadGEM helps to simulate an amount of river discharge closer to observed (e.g. Yenisey and Lena). A possible explanation could be that the scarcity of rain gauges on those basins tend to smooth rainy events during the gridding process. Further analysis will be done to assess the closure of water budget comparing the river discharge with the water vapour convergence. Also, the same experiment will be carried out by CLM forced by WFDEI and CMCC-CM2.

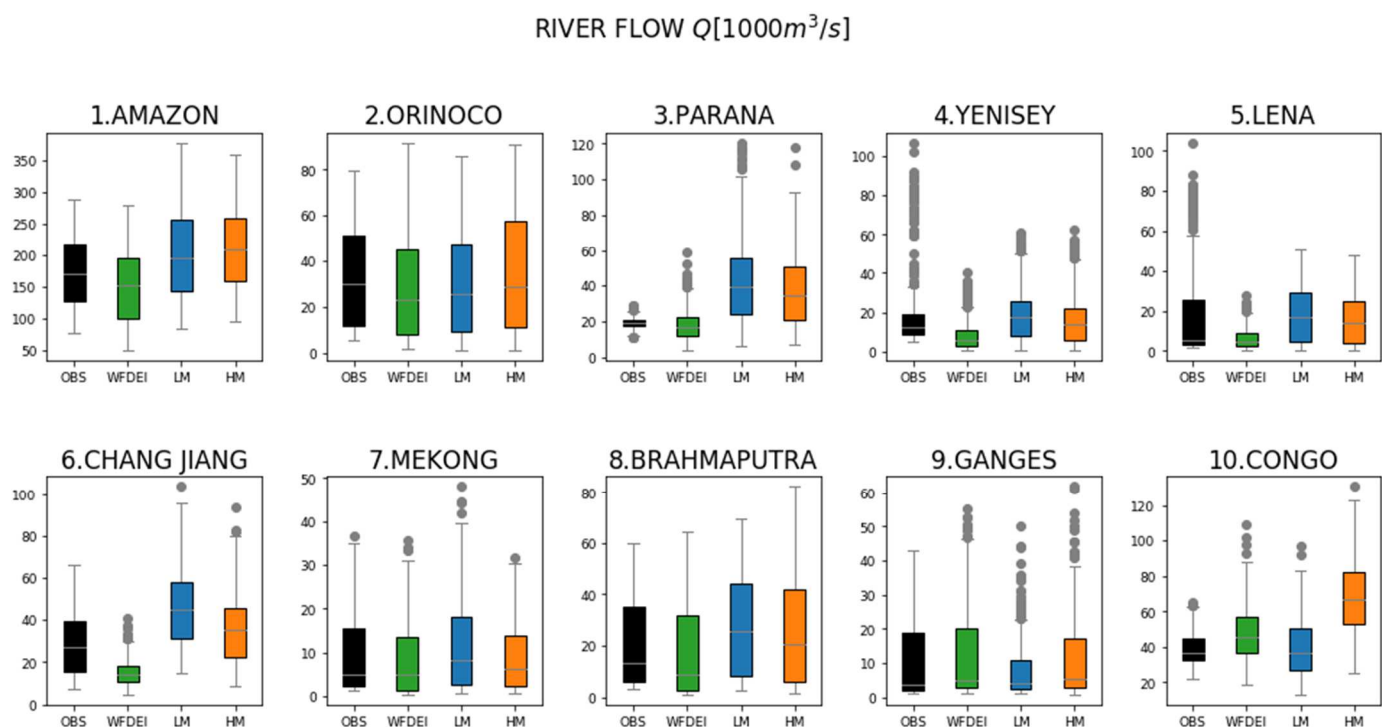


Figure 3.5.1.3. Box plots of observed and simulated river discharge with JULES forced by different datasets: WFDEI based on observations, and LM and HM based on low and high resolution HadGEM3.1 stream 1 simulations.

3.6 Stochastic Physics

3.6.1 The relative impacts of stochastic physics and resolution on extreme precipitations, mean state and North Atlantic jet (UOXF)

Previous work on the impact of increased resolution on extreme precipitation events over Europe (submitted for deliverable D2.2) showed that the representation of such extremes improved uniformly across the Stream 1 ensemble when increasing resolution. As part of extending this work further and linking it to the goals of WP4, this analysis was extended to consider the impact of stochasticity versus increased resolution. For the EC-Earth 3P model, we performed atmosphere-only simulations with and without the stochastic scheme SPPT turned on in the atmosphere. Figure 3.6.1.1 shows the result compared to GPCP satellite data. It can be seen that stochastic physics also increases the frequency of extreme precipitation over Europe, but not as much as increased resolution. In particular, for the most extreme events, SPPT is significantly outperformed by the high-resolution model, suggesting that the SPPT scheme is not effectively targeting model error in this region. Over the tropics (not shown), the scheme is more effective than high-resolution at increasing precipitation extremes (consistent with earlier studies), but tends to increase them too much relative to GPCP. Similar analysis (not shown) paints a similar picture for surface wind-speed.

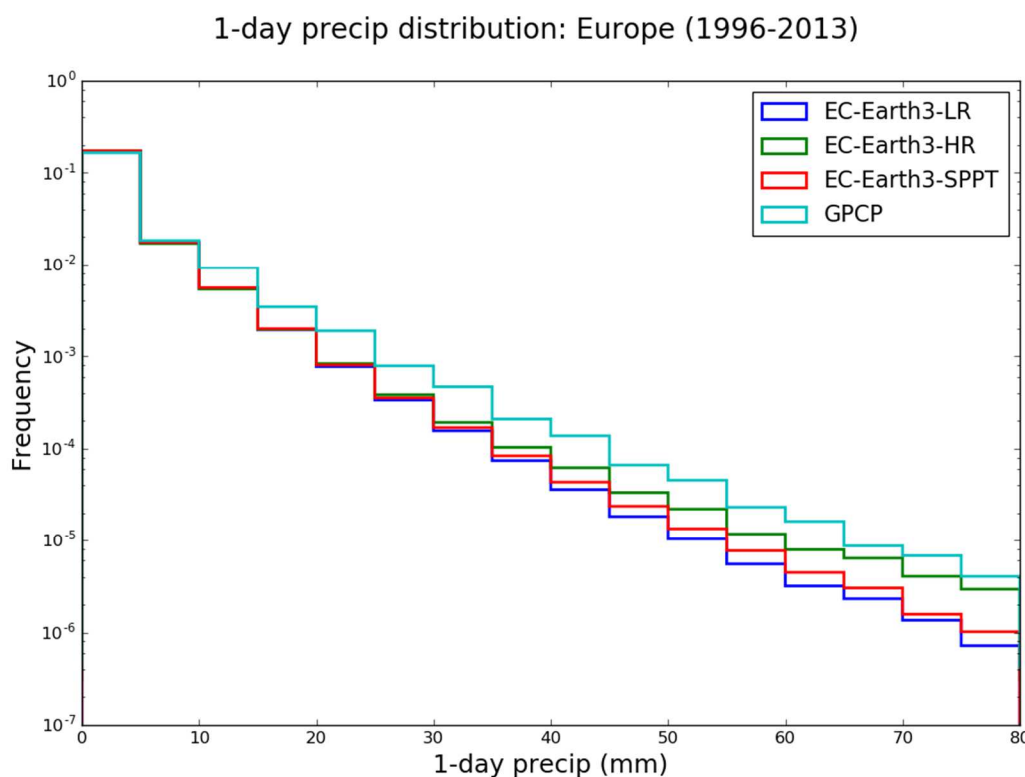


Figure 3.6.1.1. Histograms of daily precipitation over Europe (1996-2013) for the EC-Earth 3P model. Low-resolution (blue), high-resolution (green) and low-resolution+stochastic physics (red). GPCP (mauve) included as a reference. Note the logarithmic scale on the y-axis.

In the same vein, we considered the relative impact of stochastic physics schemes versus increased resolution in an ensemble of coupled simulations. We considered 4 configurations of EC-Earth: the default, deterministic version; one with the SPPT scheme on; one with stochastic ocean schemes on and one with a more flexible version of SPPT (dubbed

independent SPPT, or ISPPT) as well as stochastic land and ocean components. These are referred to as, respectively, CTRL, SPPT, OCE and PESM ('Probabilistic Earth-System Model'). An implementation paper describing these schemes and their impact on the mean state in pre-Primavera simulations is currently under review (Strommen et al., 2019). That analysis showed notable impacts on the mean state, so we have aimed to study mean state changes relative to increased resolution. Figure 3.6.1.2 shows an example of the impact of the fully stochastic configuration PESM versus resolution on surface temperature. It can be seen that the default low-resolution CTRL simulations are too warm compared to re-analysis, and both stochastic physics and resolution help to alleviate this. However, both schemes have too much cooling in the tropics, where the CTRL model is typically too cold. The HR model notably reduces the northern hemisphere warm bias, much more than any of the stochastic schemes, and the amplitude of the global mean change is much higher as well.

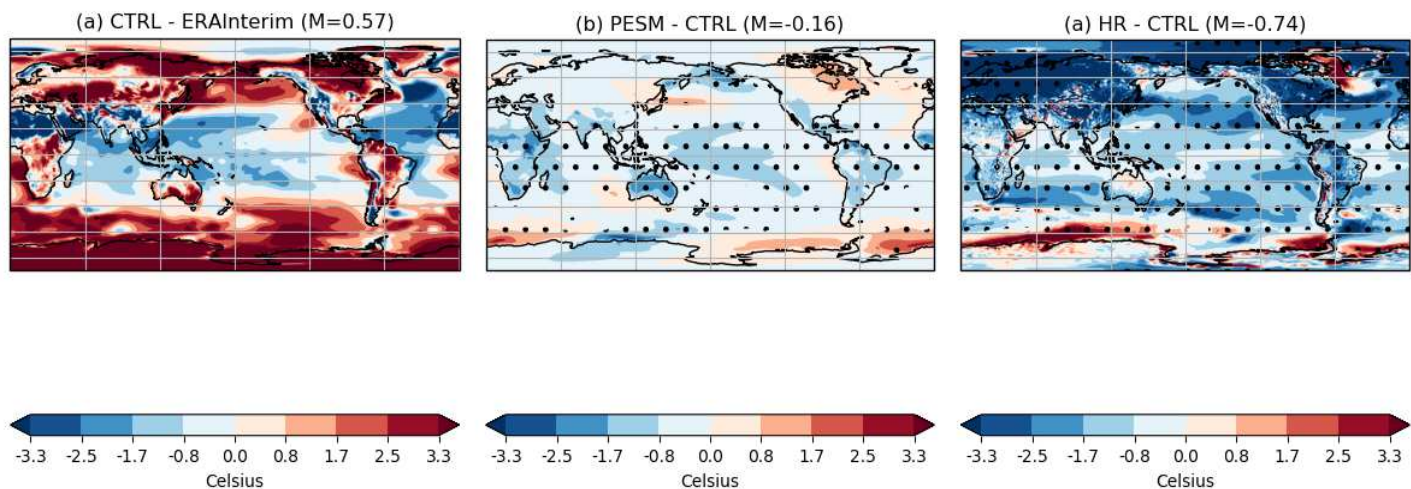


Figure 3.6.1.2. Changes in mean surface temperature (1979-2017). (a) LR deterministic CTRL simulations minus ERA-Interim re-analysis, (b) fully stochastic LR minus CTRL, (c) HR minus CTRL. Stippling indicates changes that are significant to a 90% confidence interval, determined using a two-tailed T-test.

For precipitation, seen in Figure 3.6.1.3, the stochastic schemes perform comparably to the high resolution model, with both clearly working to reduce the classic 'split ITCZ' bias in the CTRL simulations.

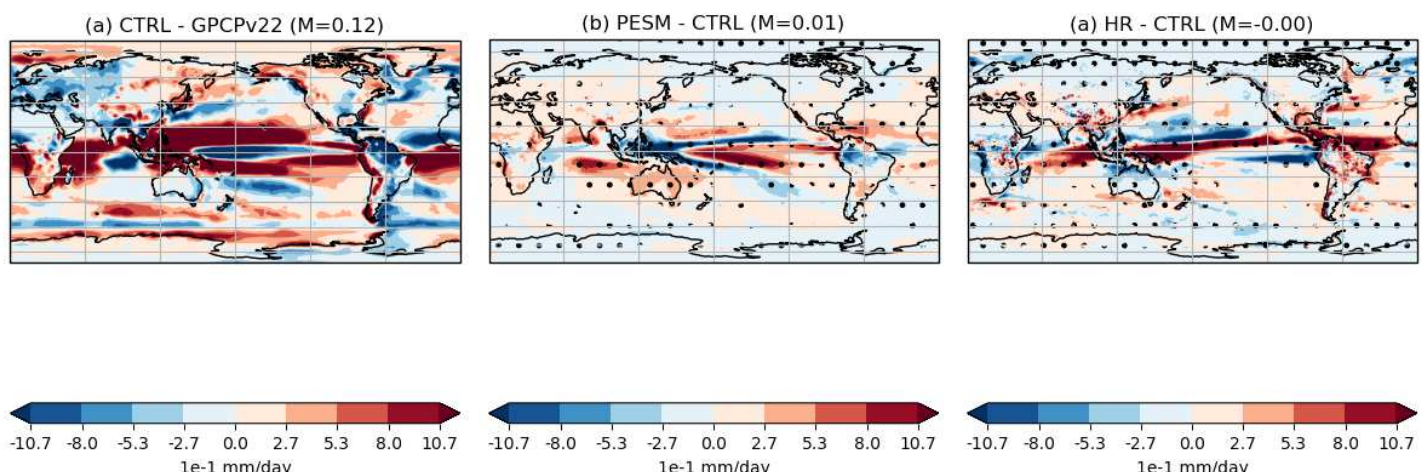


Figure 3.6.1.3. Changes in mean precipitation (1979-2017). (a) LR deterministic CTRL simulations minus ERA-Interim re-analysis, (b) fully stochastic LR minus CTRL, (c) HR minus CTRL. Stippling

indicates changes that are significant to a 90% confidence interval, determined using a two-tailed T-test.

Finally, we began examining the impact of both stochastic physics and increased resolution on the trimodal jet structure in the North Atlantic (Woolings et al. 2010). Filtered wind-fields at 850hPa were used to determine the position of the jet, and a trimodal distribution was fitted to this field. Figure 3.6.1.4 shows the observed changes. It can be seen that the CTRL simulation already has a good trimodal structure compared to re-analysis, and the stochastic schemes do not change this. However, the HR simulation appears to deteriorate the structure to an extent that appears significant compared to internal variability. This seems to be related to the fact that the HR model significantly weakens the jet, while none of the stochastic simulations do (not shown). This results in a less pronounced trimodal structure. This work will also be examined further in the next reporting period.

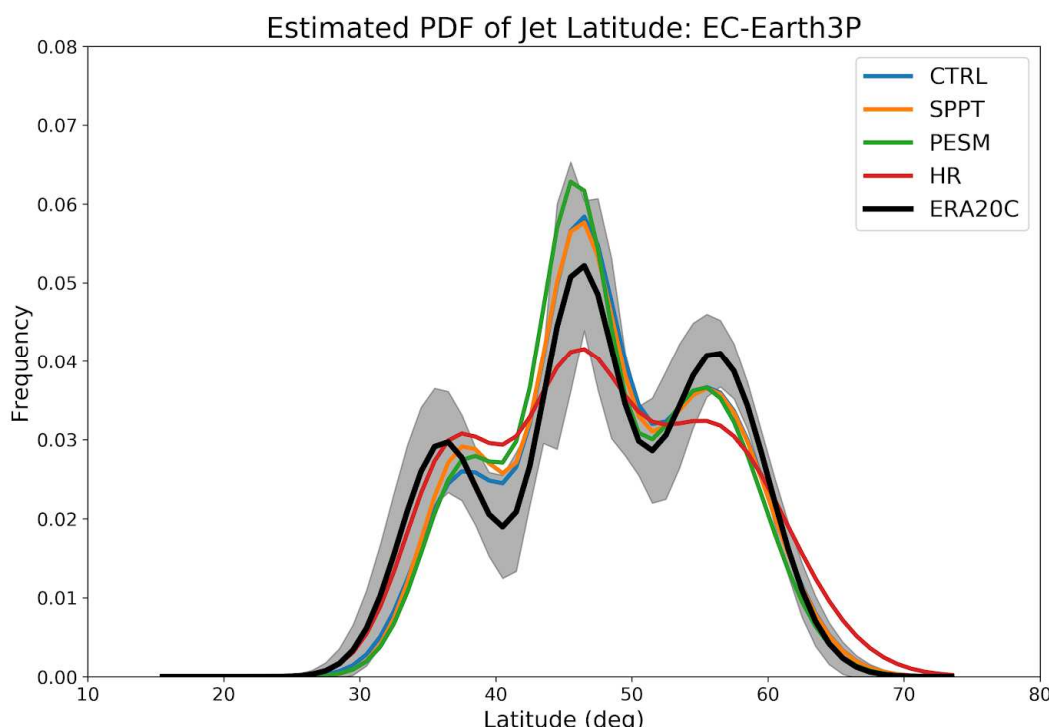


Figure 3.6.1.4. Fitted probability density functions to histograms of the jet latitude during DJF, 1950-2000. CTRL (blue), stochastic simulations (yellow, green) and HR deterministic (red). ERA20C shown in black, with shading indicating sampling variability.

To conclude, our analysis so far shows that in several respects (mean state changes and European extreme events), stochastic physics can mimic the impact of increased resolution. However, the amplitude of change is sometimes smaller with stochastic physics, suggesting that the schemes may need further tuning to represent the sub-grid scale errors better. On the other hand, increased resolution can sometimes deteriorate the model (as with the jet latitude structure) in ways that stochasticity appears not to. This shows stochasticity remains a promising alternative route to improved climate models.

3.6.2 The impact of increased resolution and stochastic physics on the representation of wintertime North-Atlantic Weather Regimes in coupled simulations (CNR)

The impact of increased resolution on the representation of Euro-Atlantic Weather Regimes (WRs) (Dawson et al., 2012) in the atmosphere-only Stream1 PRIMAVERA simulations has been included in deliverable D2.2. It was concluded that the high resolution tends to slightly improve the robustness of the regime structure, while no significant change was observed in the regime patterns. Small improvements were seen in the persistence of the Scandinavian Blocking regime, though not in all models.

We now report on the relative impacts of increased resolution and stochastic physics schemes on the representation of WRs in coupled simulations. We consider two different sets of experiments:

- the Stream 1 coupled simulations of PRIMAVERA, to assess the impacts of the increased resolution;
 - the ensemble of coupled simulations performed with EC-Earth and described in Section 3.6.1 of this deliverable, to assess the impacts of stochastic physics. The ensemble is characterized by 4 different configurations, with 3 independent simulations each: CTRL (control simulation), SPPT (SPPT in the atmosphere), OCE (stochastic physics in the ocean only) and PESM (stochastic physics in all components). Note that this set of simulations used the EC-Earth Stream 2 model version, which differs from Stream 1 for some parameters controlling the ocean turbulent kinetic energy scheme and the thermal conductivity of the snow on sea ice.

The reference dataset has been obtained merging years 1957-1978 from ERA40 and years 1979-2014 from ERA-Interim reanalyses. The Euro-Atlantic weather regimes observed in this dataset are shown in Figure 3.6.2.1. For each simulation and the reference, we considered the daily DJF 500 hPa geopotential height fields on the Euro-Atlantic region and performed a K-means clustering analysis in a reduced 4 EOF phase space. This has been done through the WRtool, thoroughly described in deliverable D1.2. The technique is also described in deliverable D2.2.

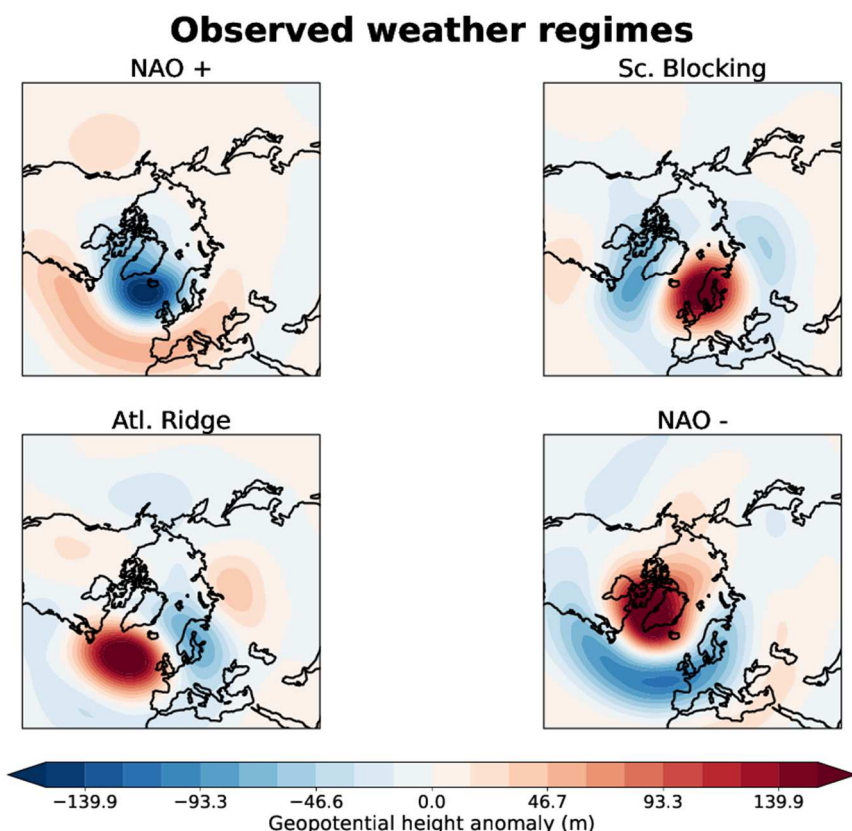


Figure 3.6.2.1. Weather Regimes on the Euro-Atlantic sector computed from ERA reanalysis relative to the 1957-2014 period (ERA40 until 1978, ERA-Interim afterwards).

The ability of the models in reproducing the WRs patterns is synthetically measured by the RMS error between the observed and simulated patterns (averaged for all patterns), shown in Figure 3.6.2.2. The RMS errors have been calculated as in Dawson and Palmer (2015). Slight improvements are seen with the increased resolution for most models (left panel). For the ensemble of simulations with the stochastic physics schemes active the result is less clear, due to the large variability inside each group (right panel). However, it seems that the SPPT configuration slightly improves the overall pattern representation with respect to the CTRL simulations. The two sets of simulations with the stochastic physics active in the ocean component (OCE and PESM) appear to slightly worsen the overall WRs patterns, although the differences are not significant.

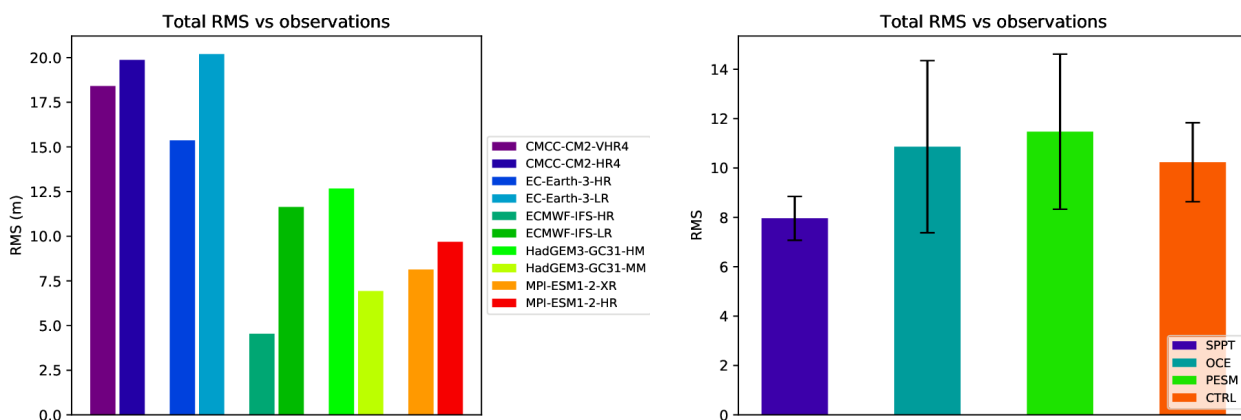


Figure 3.6.2.2. RMS error of the simulated versus observed WR pattern, averaged over all regimes. Left panel: Stream1 simulations, for each model the HR simulation is plotted on the left. Right panel: EC-Earth simulations with different configuration of the stochastic physics. Error bars are the ensembles standard deviations. Note that the CTRL configuration of EC-Earth in the right panel differs from the LR version in the left panel.

Figure 3.6.2.3 shows the bias in the frequency of occurrence of each WR, for the Stream 1 simulations (left panel) and for the EC-Earth stochastic physics ensemble (right panel). The main systematic errors are seen in the occurrence of the NAO+ regime, which is systematically underestimated in models. The occurrences of the other regimes tend to be overestimated, the Atlantic Ridge showing the strongest positive bias. No significant variation in the biases is observed with increased resolution (left panel). For the EC-Earth stochastic physics ensemble (right panel), some differences are seen between the different configurations: the CTRL configuration performs best for NAO+ and Atlantic Ridge, the SPPT for NAO- and the PESM for Scandinavian Blocking. The OCE configuration presents the largest errors overall. However, a larger number of ensemble members would be needed to reduce the intra-ensemble variability (error bars in Figure 3.6.2.3) and assess significant changes in this respect.

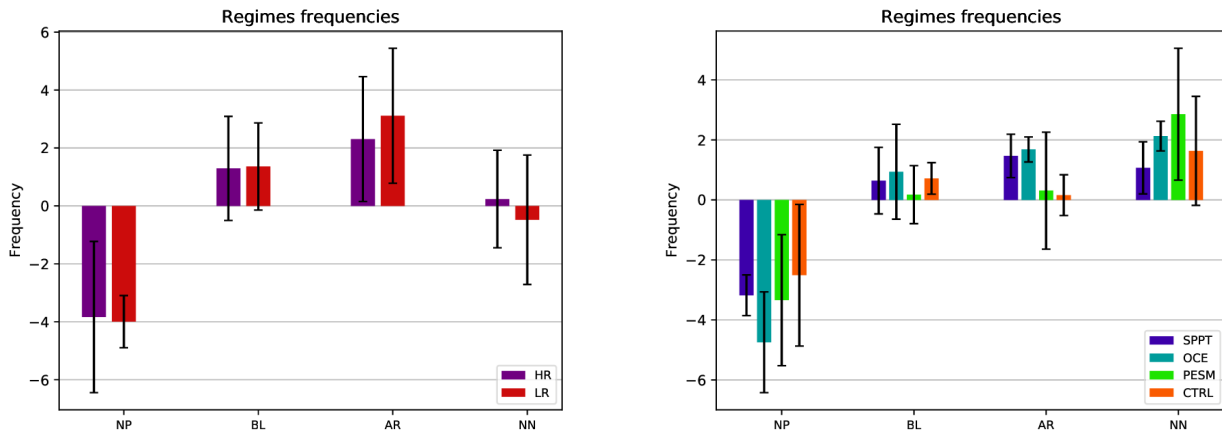


Figure 3.6.2.3. Bias of the simulated frequency of occurrence of each WR. Left panel: Stream1 simulations, multi-model averages for the increased resolution (HR) and standard resolution (LR). Right panel: EC-Earth ensemble with different configurations of the stochastic physics. The error bars represent the standard deviation inside each ensemble.

The simulated WRs' residence times statistics also show systematic differences with respect to the observations. Figure 3.6.2.4 shows the bias of the daily statistics of regime duration (bars) and a 3-day running mean (lines). The results are shown for the Stream 1 HR and LR multi-model ensembles (left panel) and for the EC-Earth CTRL and SPPT configurations (right panel). The overall tendency for models is to underestimate the 5-10 days NAO+ events, while overestimating NAO+ events shorter than 5 days. For the Atlantic Ridge the tendency in models is opposite, with underestimation of short events (< 5 days) and overestimation of 5-10 day events. Short events are overestimated also for NAO-, with slight underestimation of events lasting about 15 days. For Scandinavian Blocking the differences are generally small, with a slight overestimation of 5-10 days and underestimation of 10-15 days events. LR and HR models show the same general behavior, with small differences. This is also the case for the SPPT and CTRL EC-Earth configurations. The other configurations behave in similar manner, slightly increasing the differences for the NAO+ regime residence times (not shown).

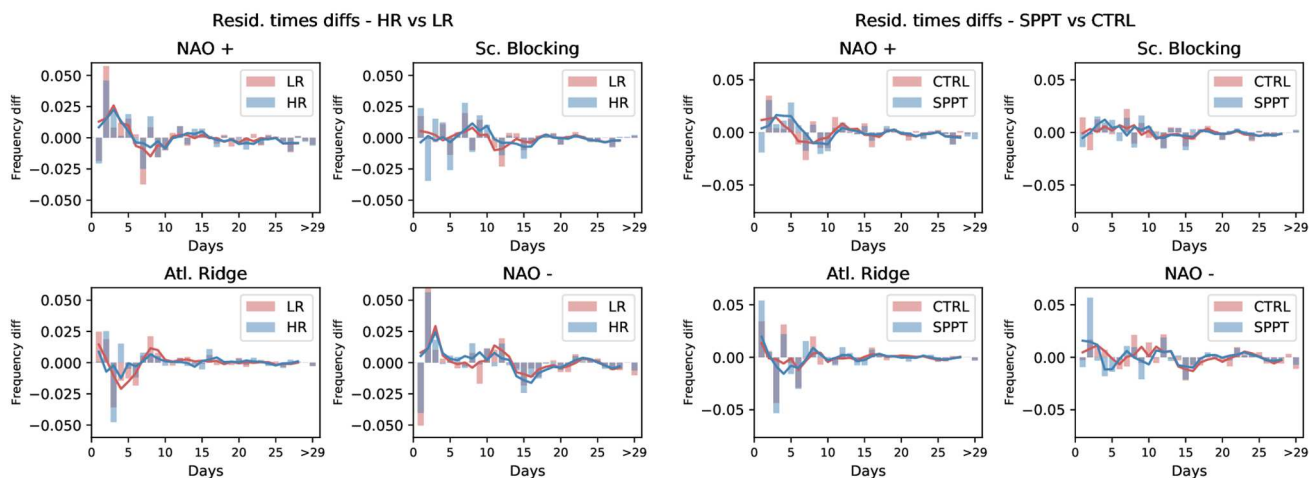


Figure 3.6.2.4. Bias of the simulated WR residence times statistics. Bars show the bias in the frequency of WR events that last a specific number of days. Lines are the 3-day running means. Left panel: Stream1 simulations, average over the HR and LR multi-model ensembles. Right panel: EC-Earth CTRL vs SPPT configuration. The other configurations show similar behaviours.

Concluding, the coupled models show yet some difficulties in correctly reproducing the observed Weather Regimes over the Euro-Atlantic sector during winter. The increased resolution slightly improves the WRs patterns for most models. The SPPT scheme in the atmosphere slightly improves the WR pattern representation, while the simulations with ocean stochastic physics (OCE and PESM) show slightly larger biases. Coupled models also present systematic biases in the WRs frequencies of occurrence and in the WRs' residence times. However it is very difficult to assess whether there are improvements due to increased resolution or stochastic physics, and further studies are needed in this direction. Both sets of simulations would need a larger number of ensemble members in order to assess if the differences are significant with respect to the intra-ensemble variability.

References

- Blanke, B., and P. Delecluse, 1993: Variability of the Tropical Atlantic Ocean Simulated by a General Circulation Model with Two Different Mixed-Layer Physics. *J. Phys. Oceanogr.*, 23 (7), 1363–1388, doi:10.1175/1520-0485(1993)023h1363:VOTTAOi2.0.CO;2.
- Berghuijs, W., Woods, R., and M Hrachowitz, 2014. A precipitation shift from snow towards rain leads to a decrease in streamflow. *Nature Climate Change* , 583-586.
- Bintanja, R., and O. Andy, 2017. Towards a rain-dominated Arctic. *Nature Climate Change* , 263-267.
- Bintanja, R., and F. Selten, 2014: Future increases in Arctic precipitation linked to local evaporation and sea-ice retreat. *Nature* , 479-482.
- Branstetter, M.L., 2001. Development of a parallel river transport algorithm and applications to climate studies. Ph.D. dissertation, University of Texas at Austin.
- Brooks, R.H. and Corey, A.T., 1964. Hydraulic Properties of Porous Media. *Hydrology Papers* 3, Colorado State University, Fort Collins, 27 p.
- Cavalieri, D. J., C. L. Parkinson, P. Gloersen, and H. J. Zwally. 1996, updated yearly. Sea Ice Concentrations from Nimbus-7 SMMR and DMSP SSM/I-SSMIS Passive Microwave Data, Version 1. Boulder, Colorado USA. NASA National Snow and Ice Data Center Distributed Active Archive Center.
- Clapp, R.B., and Hornberger, G.M. 1978. Empirical equations for some soil hydraulic properties. *Water Resour. Res.* 14:601-604
- Dawson A., Palmer T., Corti S., 2012. Simulating regime structures in weather and climate prediction models. *Geophysical Research Letters*, doi:10.1029/2012GL053284
- Dawson A. and Palmer T., 2015. Simulating weather regimes: impact of model resolution and stochastic parameterization. *Clim Dyn*, doi:10.1007/s00382-014-2238-x
- Dussin, R., Barnier, B., Brodeau, L., and J. M. Molines, 2016: DRAKKAR FORCING SET DFS5.
- EC EARTH, 2009: Info on EC EARTH. Retrieved 2017 6-November from EC EARTH: <https://www.ec-earth.org/>
- Eden, C., and R. J. Greatbatch, 2008: Diapycnal mixing by meso-scale eddies. *Ocean Model.*, 23, 113–120, doi:10.1016/j.ocemod.2008.04.006.
- EUMETSAT SAF on Ocean and Sea Ice, 2016. Global Sea Ice Concentration climate data record release 1.1 (period 1978-2009) - DMSP. OSI SAF. DOI: 10.15770/EUM_SAF_OSI_0001
- Forbes, R., and A. Tompkins, 2011. An improved representation of cloud and precipitation. *ECMWF Newsletter* , 13-18.
- Holden, J., 2012. An Introduction to Physical Geography and the Environment. Harlow: Pearson Education Limited.
- Gaspar, P., Y. Grégoris, and J.-M. Lefevre, 1990. A simple eddy kinetic energy model for simulations of the oceanic vertical mixing: Tests at station Papa and long-term upper ocean study site. *J. Geophys. Res. Oceans*, 95 (C9), 16179–16193, doi:10.1029/JC095iC09p16179.

Global Soil Data Task. 2014. Global Soil Data Products CD-ROM Contents (IGBP-DIS). Data Set. Available online [<http://daac.ornl.gov>] from Oak Ridge National Laboratory Distributed Active Archive Center, Oak Ridge, Tennessee, U.S.A. <http://dx.doi.org/10.3334/ORNLDAAAC/565>.

Goessling, H. F., S. Tietsche, J. J. Day, E. Hawkins, and T. Jung, 2016. Predictability of the Arctic sea ice edge, *Geophys. Res. Lett.*, 43, 1642–1650, doi:10.1002/2015GL067232.

Griffies, S. M., Levy, M., Adcroft, A. J., Danabasoglu, R., Hallberg, R. W., Jacobsen, D., Large, W., Ringler, T. D., 2013. Theory and numerics of the Community Ocean Vertical Mixing (CVMix) Project. Tech. rep, <https://gitub.com/CVMix/CVMix-description>.

Gutjahr, O., Putrasahan, D., Lohmann, K., Jungclaus, J. H., von Storch, J.-S., Haak, H., and Stössel, A., 2018. Max Planck Institute Earth System Model (MPI-ESM1.2) for High-Resolution Model Intercomparison Project (HighResMIP). *Geosc. Mod. Dev. Discuss.*, doi: 10.5194/gmd-2018-286.

Hersbach, H, de Rosnay, P, Bell, B, Schepers, D, Simmons, A, Soci, C, Abdalla, S, Alonso-Balmaseda, M, Balsamo, G, Bechtold, P, Berrisford, P, Bidlot, J-R, de Boisséson, E, Bonavita, M, Browne, P, Buizza, R, Dahlgren, P, Dee, D, Dragani, R, Diamantakis, M, Flemming, J, Forbes, R, Geer, AJ, Haiden, T, Hólm, E, Haimberger, L, Hogan, R, Horányi, A, Janiskova, M, Laloyaux, P, Lopez, P, Munoz-Sabater, J, Peubey, C, Radu, R, Richardson, D, Thépaut, J-N, Vitart, F, Yang, X, Zsótér, E, Zuo, H, 2018, Operational global reanalysis: progress, future directions and synergies with NWP, ERA Report Series Number27

Hewitt, H. T., M. J. Roberts, P. Hyder, T. Graham, J. Rae, S. E. Belcher, R. Bourdallé-Badie, D. Copsey, A. Coward, C. Guiavarch, C. Harris, R. Hill, J. J.-M. Hirschi, G. Madec, M. S. Mizielski, E. Neininger, A. L. New, J.-C. Rioual, B. Sinha, D. Storkey, A. Shelly, L. Thorpe, and R. A. Wood, 2016. The impact of resolving the Rossby radius at mid-latitudes in the ocean: results from a high-resolution version of the Met Office gc2 coupled model, *Geoscientific Model Development*, 9(10), 3655–3670, doi:10.5194/gmd-9- 3655-2016.

Keeley, S.P.E, R.T. Sutton, L.C. Shaffrey, 2012, The impact of North Atlantic sea surface temperature errors on the simulation of North Atlantic European region climate, *Quarterly Journal of the Royal Meteorological Society*, 138, 1774-1783

Large, W. G., J. C. McWilliams, and S. C. Doney, 1994: Oceanic vertical mixing: A review and a model with a nonlocal boundary layer parameterization. *Rev. Geophys.*, 21 (4), 363–403, doi:10.1029/94RG01872.

Liu, J., Curry, J., Wang, H., Song, M., and R. Horton, 2012: Impact of declining Arctic sea ice on winter snowfall. *Proc. Natl Acad. Sci.* , 4074-4079.

Marzocchi, A., J. J. M. Hirschi, N. P. Holliday, S. A. Cunningham, A. T. Blaker, and A. C. Coward, 2015. The north Atlantic subpolar circulation in an eddy-resolving global ocean model, *J. Mar. Syst.*, 142, 126–143, doi:10.1016/j.jmarsys.2014.10.007.

Massonet F., Barthelemy A., Worou, K., Fichefet T., Vancopenolle, M., Rousset, C. and E. Moreno-Chamarro, 2019: Insights on the discretization of the ice thickness distribution in the NEMO3.6-LIM3 global ocean-sea ice model (Under review). *Geoscientific Model Development*.

Mauritsen, T., Bader, J., Becker, T., and Coauthors, 2019: Developments in the MPI-M Earth System Model version 1.2 (MPI-ESM 1.2) and its response to increasing CO₂. *J. Adv. Model. Earth Syst.*, doi: 10.1029/2018MS001400.

McCoy, D. T., Field, P. R., Elsaesser, G. S., Bodas-Salcedo, A., Kahn, B. H., Zelinka, M. D., Kodama, C., Mauritsen, T., Vanniere, B., Roberts, M., Vidale, P. L., Saint-Martin, D., Voldoire, A., Haarsma, R., Hill, A., Shipway, B., and Wilkinson, J.: Cloud feedbacks in extratropical cyclones: insight from long-term satellite data and high-resolution global simulations, *Atmos. Chem. Phys.*, 19, 1147-1172, <https://doi.org/10.5194/acp-19-1147-2019>, 2019.

Montzka, C., Herbst, M., Weihermüller, L., Verhoef, A. and Vereecken, H., 2017. A global data set of soil hydraulic properties and sub-grid variability of soil water retention and hydraulic conductivity curves. *Earth System Science Data*, 9 (2). pp. 529-543. ISSN 1866-3516

Müller, W.A., Jungclaus, J. H., Mauritsen, T., and Coauthors, 2018: A higher-resolution version of the Max Planck Institute Earth System Model (MPI-ESM1.2-HR), *J. Adv. Model. Earth Syst.*, 9, doi: 10.1029/2017MS001217.

Oki, T., T. Nishimura, and P. Dirmeyer, 1999. Assessment of annual runoff from land surface models using Total Runoff Integrating Pathways (TRIP). *Journal of the Meteorological Society of Japan*, 77 (1B), pp. 235-255.

Olbers, D., and C. Eden, 2013: A Global Model for the Diapycnal Diffusivity Induced by Internal Gravity Waves. *J. Phys. Oceanogr.*, 43 (8), 1759–1779, doi:10.1175/JPO-D-12-0207.1.

Pacanowski, R. C., and S. G. H. Philander, 1981: Parameterization of Vertical Mixing in Numerical Models of Tropical Oceans. *J. Phys. Oceanogr.*, 11 (11), 1443–1451, doi:10.1175/1520-0485(1981)011h1443:POVMINi2.0.CO;2.

Pollmann, F., C. Eden, and D. Olbers, 2017: Evaluating the Global Internal Wave Model IDEMIX Using Finestructure Methods. *J. Phys. Oceanogr.*, 47, 2267–2289, doi:10.1175/JPO-D-16-0204.1.

PRIMAVERA, 2015. *Objectives of PRIMAVERA*. Retrieved 2017 2-October from PRIMAVERA: <https://www.primavera-h2020.eu>

Roberts, C.D., R. Senan, F. Molteni, S.Boussetta, M.Mayer, S.P.E. Keeley, 2018, Climate model configurations of the ecmwf integrated forecasting system (ecmwf-ifs cycle 43r1) for highresmip, *Geoscientific Model Development*, 11, 3681–3712, 2018

Roberts, M. J., P. L. Vidale, C. Senior, and Coauthors, 2018. The benefits of global high-resolution for climate simulation: process-understanding and the enabling of stakeholder decisions at the regional scale, *BAMS*, 99(11), 2341-2359.

Screen, J., and I. Simmonds, 2012. Declining summer snowfall in the Arctic: causes, impacts and feedbacks. *Climate Dynamics* , 2243-2256.

Strommen, K. and Co-authors, 2019: Introducing the Probabilistic Earth-System Model: Examining The Impact of Stochasticity in EC-Earth v3.2, *Geoscientific Model Development Discussions*, under review.

Thomas, M. A., Devasthale, A., Koenigk, T., Wyser, K., Roberts, M., Roberts, C., and Lohmann, K.: A statistical and process oriented evaluation of cloud radiative effects in high resolution global models, *Geosci. Model Dev. Discuss.*, <https://doi.org/10.5194/gmd-2018-221>, in review, 2018.

Våge, K., Pickart, R., Sarafanov, A., and Co-authors, 2011: The Irminger Gyre: circulation, convection, and interannual variability. Deep-Sea Res. I, 58, 590–614, doi:10.1016/j.dsr.2011.03001.

Vanniere, B., P. L. Vidale, M.-E. Demory, and Coauthors, 2018. Multi-model evaluation of the sensitivity of the global energy budget and hydrological cycle to resolution. Climate Dynamics, 1-30.

Wang, Q., Wekerle, C., Danilov, S., Wang, X., and Jung, T., 2018: A 4.5 km resolution Arctic Ocean simulation with the global multi-resolution model FESOM1.4, Geosci. Model. Dev., 11, 1229-1255, doi: 10.5194/gmd-11-1229-2018.

Weedon, G. P., G. Balsamo, N. Bellouin, S. Gomes, M. J. Best, and P. Viterbo, 2014. The WFDEI meteorological forcing data set: WATCH Forcing Data methodology applied to ERA-Interim reanalysis data, Water Resour. Res., 50, 7505–7514, doi:10.1002/2014WR015638.

Woollings, T., Hannachi, A., & Hoskins, B., 2010. Variability of the North Atlantic eddy-driven jet stream. Quarterly Journal of the Royal Meteorological Society, 136, 856–868.

Zuo, H, Alonso-Balmaseda, M, Mogensen, K, Tietsche, S, 2018, OCEAN5: The ECMWF Ocean Reanalysis System and its Real-Time analysis component, ECMWF Technical Memorandum Number 823.

4. Lessons Learnt

4.1. The relative merits of enhanced model resolution versus model developments on bias reduction.

The relatively limited set of processes, and narrow range of spatial resolutions analysed in this report does not allow making conclusive statements on the relative merits of resolution and improved parameterizations on the overall models behavior. Most importantly, the lack of a systematic implementation and testing of specific physics improvements across different models prevents to address the model dependency of the results presented.

However, despite the above limitations, a few indications emerge, calling for more in-depth analyses to corroborate the findings of this deliverable. These are reported below.

A significant aspect emerging from this set analyses is the strong regional and process dependence of the relative benefits (in terms of bias reduction) of resolution and improved physics.

Biases in the upper thermal structure of the North Atlantic (SST and stratification) appear to benefit more from a resolution increase, than from the use of more sophisticated vertical mixing schemes (IDEMIX and OSMOSIS; 3.2.1 and 3.2.2, respectively). However, the opposite is true for the Southern Ocean, where the use of the OSMOSIS mixing scheme is found to significantly alleviate a long-lasting warm austral summer SST bias (3.2.2), which, on the other hand, appears to be relatively insensitive to increases in the resolution (Hewitt et al., 2016). In another analysis (3.3.2), changes in a set of ocean model parameters (affecting, among other aspects, the penetration of turbulent kinetic energy below the mixed layer and the Langmuir cells representation) are conducive to a systematic reduction in the integrated ice edge error over the Arctic, while increasing resolution yields a more uncertain result.

A case study providing a particularly clear response to the primary issue addressed by D2.3, is the analysis presented in section 3.4.1, focusing on the hydrological cycle over the Arctic. Here it is shown how a refined representation of the snowfall ratio (the ratio of snowfall to total precipitation) can lead to a stronger improvement compared to the mere increment of model resolution.

In other cases, the assessment of the relative impacts of resolution enhancement and improved physics yields more elusive results. This is the case of the analysis presented in section 3.3.1, testing the inclusion of Arctic melt ponds against the increase of model resolution. According to this set of results (based on EC-Earth) melt ponds and increased resolution lead to a similar improvement of sea ice concentrations in the Barents Sea and a reduced cold bias in the near-surface temperatures over the Arctic. Analogous indications of a substantially equivalent impact of model physics and resolution on the representation of the Arctic climate can be drawn from the analyses presented in section 3.3.3, based on the ECMWF climate model. However, significant differences emerge when looking at the European surface climate (surface temperatures and precipitation), showing a prevailing effect of resolution.

An intriguing aspect emerging for a specific subset of the analysed physical processes, is the potential interdependency of model resolution and physics complexity. This is the case for radiative fluxes, clouds, and aerosol-cloud interactions (3.4.2). There are benefits from increasing resolution for simulating clouds, aerosols, and radiation, but those benefits may require very high resolutions to fully appear. Those benefits are also modulated by the complexity in model physics. Complex cloud microphysics help make the most of very high resolutions (e.g., in terms of simulating cloud water content in extratropical cyclones).

Similarly, simplifying the representations of aerosol-cloud interactions offsets some of the gains of increasing resolution when simulating cloud cover and albedo.

The analysis of the relative impact of stochastic physics versus increased resolution (3.6) contributes to enlarge the scope of D2.3 beyond the mere enhancement of physics complexity via the inclusion of more sophisticated (compared to standard model configurations) physical parameterizations.

The analyses presented in section 3.6.1 show that in several respects (mean state changes and European extreme events), stochastic physics can mimic the impact of increased resolution. However, the amplitude of change is sometimes smaller with stochastic physics, suggesting that the schemes may need further tuning to represent the sub-grid scale processes with better fidelity. On the other hand, increased resolution can sometimes deteriorate the model (as with the jet latitude structure) in ways that stochasticity appears not to. The representation of winter weather regime patterns in the North Atlantic (3.6.2) exhibits a slight improvement associated with increased resolution, while a similar bias reduction is only achieved when stochastic physics is applied to the atmospheric component, while a worsening of the biases is obtained when ocean stochastic physics is used. Overall, stochasticity remains a promising avenue for improving climate models, but a robust assessment of its merits with respect to resolution will require large-sized ensembles of simulations to verify the significance of the detected differences against the intra-ensemble variability.

4.2 Recommendations for Stream 2

An expected outcome of D2.3 was the delivery of recommendations to WP6 for the design of Stream 2 (S2) simulations. However, during the project course, concerns have emerged within the PRIMAVERA partnership regarding the potential lack of robustness of Stream 1 (S1) results, due to the low dimensionality of the simulation ensembles (only a few groups were able to contribute with multiple members to S1 integrations), leading in turn to a poor constrain of simulated internal variability. This concern triggered extensive discussions between project PIs, work package leaders and lead representatives of the participating groups, culminated in a dedicated intra-model workshop (held in Amsterdam, on 12 November 2018). Following the decisions taken at the workshop, the initial plan for S2 simulations underwent a substantial re-design, to account for the above mentioned concerns. In the original plan (outlined in the PRIMAVERA document of work) S2 was expected to deliver a set of simulations done with the model developments tested as part of the WP2 and WP3 activities with input from WP11 from user requirements. After the workshop in Amsterdam, PRIMAVERA partners agreed on a revised S2 set, where major emphasis was given to the strengthening of S1 reliability through the delivery of additional ensemble members for the WP6 flagship simulations. Moreover, due to the postponement of D2.3 (after the 9-month project extension, from month 34 to month 40), the present report is delivered after decisions have been taken on the S2 design. However, it must be mentioned that some of the analyses reported in D2.3 were actually completed before the meeting in Amsterdam and their outcomes contributed to the decision of performing additional S1 ensemble members as part of S2.

All the above considered, the initial objectives of D2.3 have been revised accordingly, and no recommendations for S2 are delivered in this report – this was instead achieved via milestone MS7.

5. Links Built

The analyses presented in this report are largely based on a wide range of sensitivity experiments performed within the WP3 (improved physical parameterizations; sections 3.2-3.5) and WP4 (stochastic physics, section 3.6) groups. As such, the inferred outcomes of D2.3 analyses are complementary to the evaluations presented in D2.1 and D2.2 (assessing the impact of ocean and atmospheric model resolution, based on Stream 1 results), and contribute to create a strong linkage across WP2, WP3 and WP4.